Axonal $GABA_A$ stabilises excitability in unmyelinated sensory axons secondary to NKCC1 activity

Veronica Bonalume[1], Lucia Caffino[1], Luca F. Castelnovo[1,2], Alessandro Faroni[3], Sheng Liu[4], Jing Hu[4], Marco Milanese[5], Giambattista Bonanno[5,6], Kyra Sohns[8], Tal Hoffmann[7], Roberto De Col[8], Martin Schmelz[8], Fabio Fumagalli[1], Valerio Magnaghi[1] and Richard Carr[8]

[1]*Department of Pharmacological and Biomolecular Sciences, Università degli Studi di Milano, 20133 Milan, Italy.*

[2]*Marine Science Institute, University of Texas at Austin, Port Aransas (TX) 78373, United States.*

[3]*Blond McIndoe Laboratories, Division of Cell Matrix Biology and Regenerative Medicine, Faculty of Biology, Medicine and Health, The University of Manchester, M13 9PL Manchester, United Kingdom.*

[4]*Institute of Pharmacology, Heidelberg University, 68167 Mannheim, Germany.*

[5] *Department of Pharmacy (DIFAR), Pharmacology and Toxicology Unit, Università degli Studi di Genova, Italy*

[6]*Istituto di Ricovero e Cura a Carattere Scientifico (IRCCS), Ospedale Policlinico San Martino, Genoa, Italy*

[7]*Institute for Physiology and Pathophysiology, Friedrich-Alexander University, Erlangen, Germany*

[8]*Experimental Pain Research, Medical Faculty Mannheim, Heidelberg University, Mannheim, Germany.*

Corresponding authors:

R.C., Richard Carr: Experimental Pain Research, Medical Faculty Mannheim, University Heidelberg, Ludolf-Krehl-Str.13-17, 68167 Mannheim, Germany; richard.carr@medma.uni-heidelberg.de

V.M., Valerio Magnaghi: Department of Pharmacological and Biomolecular Sciences - University of Milan, Via G. Balzaretti 9, 20133 Milan, Italy; valerio.magnaghi@unimi.it

This is an Accepted Article that has been peer-reviewed and approved for publication in The Journal of Physiology, but has yet to undergo copy-editing and proof correction. Please cite this article as an 'Accepted Article'; doi: 10.1113/JP279664.

Key points:

- GABA depolarized sural nerve axons and increased the electrical excitability of C-fibres via $GABA_AR$.
- Axonal excitability responses to GABA increased monotonically with the rate of action potential firing.
- Action potential activity in unmyelinated C-fibres is coupled to NKCC1 loading of axonal chloride.
- Activation of axonal $GABA_AR$ stabilised C-fibre excitability during prolonged low frequency (2.5 Hz) firing.
- NKCC1 maintains intra-axonal chloride to provide feed-forward stabilisation of C-fibre excitability and thus support sustained firing.

Abbreviations

ALLO, allopregnanolone; CAP, compound action potential; C-CAP, C-fibre compound action potential; CNS, central nervous system; DAPI 4,6-diamidino-2-phenylindole; DMSO, dimethyl sulfoxide; DRG, dorsal root ganglia; GABA, γ-aminobutyric acid; $GABA_A$, GABA type A receptor; $GABA_B$, GABA type B receptor; HEPES, 4-(2-hydroxyethyl)-1-piperazineethanesulfonic acid; H-NF, heavy neurofilament; HPLC, high performance liquid chromatography; IFL, immunofluorescence; KCC2, K-Cl co-transporter type 2; NKCC1, Na-K-Cl cotransporter type 1; PFA, paraformaldehyde; PGE_2, prostaglandin E_2; THIP, 4,5,6,7-tetrahydroisoxazolo (5,4-c)pyridin-3(-ol), gaboxadol; TTX, tetrodotoxin; WT, wildtype.

Abstract

$GABA_AR$ mediated depolarisation of DRG axonal projections in the spinal dorsal horn is implicated in pre-synaptic inhibition. Inhibition, in this case, is predicated on an elevated intra-axonal chloride concentration and a depolarizing GABA response. We report here that the peripheral axons of DRG neurons are also depolarised by GABA and this results in an increase in the electrical excitability of unmyelinated C-fibre axons. $GABA_AR$ agonists increased axonal excitability while GABA excitability responses were blocked by $GABA_AR$ antagonists and were absent in mice lacking the $GABA_AR$ β3 subunit selectively in DRG neurons ($Advillin^{Cre}$ or sns^{Cre}). Under control conditions, excitability responses to GABA became larger at higher rates of electrical stimulation (0.5 - 2.5 Hz). However, during NKCC1 blockade electrical stimulation rate did not affect GABA response size, suggesting that NKCC1 regulation of axonal chloride is coupled to action potential firing. To examine this, activity-dependent conduction velocity slowing (ADS) was used to quantify C-fibre excitability loss during 2.5 Hz challenge. ADS was reduced by $GABA_AR$ agonists and exacerbated by either $GABA_AR$ antagonists, β3 deletion or NKCC1 blockade. This illustrates that activation of $GABA_AR$ stabilises C-fibre excitability during sustained firing. We posit that NKCC1 acts in a feed-forward manner to maintain an elevated intra-axonal chloride in C-fibres during ongoing firing. The resulting chloride gradient can be utilised by $GABA_AR$ to stabilise axonal excitability. The data imply that therapeutic strategies targeting axonal chloride regulation at peripheral loci of pain and itch may curtail aberrant firing in C-fibres.

Introduction

$GABA_A$ receptors ($GABA_AR$) mediate fast synaptic inhibition in mature neurons that maintain a low intracellular chloride concentration. In this case, GABA inhibition results from chloride (Cl^-) influx, i.e. outward current, and thus membrane hyperpolarization (Ben-Ari, 2002). In the majority of mature neurons, intracellular chloride is regulated dynamically by the activity of chloride transporters. Na-K-Cl cotransporter type 1 (NKCC1) mediates inward chloride transport while K-Cl co-transporter type 2 (KCC2) is the predominant outward chloride transporter (Ben-Ari, 2002). In vitro recordings indicate that KCC2 expression is low in immature neurons resulting in an elevated intracellular Cl^- concentration and thus inward depolarizing $GABA_A$ currents (Gao & van den Pol, 2001; Ben-Ari, 2002). Similarly, an elevated intracellular Cl^- concentration persists into maturity in somatosensory neurons in trigeminal (Schobel *et al.*, 2012) and spinal ganglia (DRG) (Alvarez-Leefmans *et al.*, 1988; Kaneko, 2002), in post-ganglionic sympathetic neurons (Ballanyi & Grafe, 1985) as well as in olfactory sensory neurons (Kaneko *et al.*, 2004). In DRG neurons, NKCC1 activity maintains an elevated intracellular chloride concentration (Rocha-Gonzalez *et al.*, 2008) while expression of outward Cl^- transporters, including KCC2, is low or absent (Lu *et al.*, 1999; Rivera *et al.*, 2005; Toyoda *et al.*, 2005; Gilbert *et al.*, 2007).

$GABA_A$ receptors are pentameric ligand-gated ion channels permeable to Cl^- and bicarbonate anions. Nineteen mammalian $GABA_A$ subunits, $\alpha 1–6$, $\beta 1–3$, $\gamma 1–3$, δ, ε, π, θ and $\rho 1–3$ are recognised while functional receptors are formed mostly as $\alpha 1/2\beta 2/3\gamma 2$ $GABA_A$ postsynaptically and $\alpha 4\beta 3\delta$, $\alpha 5\beta 3\gamma 2$ and $\alpha 1\beta\delta$ at extrasynaptic locations including axons (Hannan *et al.*, 2019). $GABA_AR$ subunit composition influences ligand sensitivity, channel kinetics, desensitization and spatial distribution within neurons (Mitchell *et al.*, 2008). In adult DRG neurons, $\beta 3$ is the most abundant $GABA_AR$ subunit (Ma *et al.*, 1993; Faroni *et al.*, 2019) and conditional deletion of $GABA_AR\,\beta 3$ substantially reduced depolarizing GABA currents in DRG neuronal somata (Chen *et al.*, 2014). $GABA_AR\,\beta 3$ has also been identified immunohistochemically in the presynaptic terminals of primary afferent neurons in the spinal dorsal horn (Zeilhofer *et al.*, 2012; Orefice *et al.*, 2016). Consistent with this, dorsal root potentials evoked by electrical stimulation at C-fibre intensity were absent in mice lacking $\beta 3$ (Zimmerman *et al.*, 2019).

GABA depolarizes the central terminals of adult DRG primary afferents in the ventral (Rudomin & Schmidt, 1999) and dorsal horn (Bardoni *et al.*, 2013; Chen *et al.*,

2014).Similarly, application of GABA to acutely isolated DRG somata also produces depolarizing inward currents (Zhang *et al.*, 2015; Du *et al.*, 2017) with chloride reversal potentials of around -31 mV (Kaneko, 2002). Likewise, the peripheral axons of DRG neurons respond to GABA with depolarization (Brown & Marsh, 1978; Bhisitkul *et al.*, 1987; Jackson *et al.*, 1992). However, the physiological role of axonal $GABA_AR$ has not been at all clear.

Here we used conditional deletion and pharmacology to confirm the presence of functional $GABA_AR$ along peripheral unmyelinated axons of somatosensory neurons. GABA depolarised sural nerve axons and this was accompanied by an increase in the electrical excitability of C-fibres. Axonal excitability responses to GABA increased with increasing rates of background electrical stimulation and this effect was mediated by a coupling of action potential firing to NKCC1 activity. The data establish that NKCC1 maintains an elevated intra-axonal chloride concentration during action potential activity, thus allowing chloride conductances to stabilise axonal excitability and sustain firing in unmyelinated axons.

Methods

Ethical Approval

Experiments were carried out in compliance with guidelines for the welfare of experimental animals as stipulated by the Federal Republic of Germany (Heidelberg University), the Animal Research Committee (University of Milan), and conform to the principles and regulations as described by Grundy (2015). In each case, ethics approvals were issued in accordance with the European regulations concerning care and use of animals; Council Directive 2010/63/EU of the European Parliament and the Council of 22 September 2010 on the protection of animals used for scientific purposes. Approval for animal use was provided under I-19/05 at the Medical Faculty Mannheim, Heidelberg University.

Animals

Only male mice were used. Wildtype (WT) C57BL/6N outbred mice were purchased from Charles River Laboratories (Écully, France). Mice with conditional deletion of the *gabrb3* gene encoding the β3 subunit of $GABA_AR$ were generated by crossing $Gabrb3^{fl/fl}$ (JacksonLabs#008310) with either $Advillin^{Cre}$ (Zurborg *et al.*, 2011) or $Scn10a^{Cre}$ (Agarwal *et al.*, 2004). The resulting $Advillin^{Cre};Gabrb3^{fl/fl}$ and $Scn10a^{Cre};Gabrb3^{fl/fl}$ lines are referred to here as $Adv^{Cre};$β3 and $sns^{Cre};$β3 respectively. Progeny from both lines were viable and lacked overt sensory or motor deficits. Littermate comparisons comprised combinations of either

Advillin^{Cre} or *scn10a*^{Cre} or *Gabrb3*$^{fl/fl}$ mice. Recordings from any of these genotypes together with genuine WT mice were pooled and are referred to here as "control" mice.

Anaesthesia and housing

Mice were anaesthetised with volatile anaesthetic before being killed by cervical dislocation. Anaesthetic depth was monitored by corneal blink and hind paw withdrawal reflexes. Mice were housed in ventilated polycarbonate cages (GM500SU, Tecniplast, Hohenpeissenberg, Germany) in a controlled environment at 20°C with a 12-hour light dark cycle and with access to food and water ad libitum.

Sural nerve preparation

After mice were killed (see Anaesthesia and Housing) both sural nerves were removed rapidly by dissection over a length of approximately 1.5 cm and the ensheathing epineurium was removed gently to facilitate drug permeation. Desheathed nerves were mounted between two glass pipettes in an organ bath (Fig. 1A). Each end of the nerve was drawn into a glass pipette and sealed in position with vaseline to establish a mechanical seal and a high resistance electrical seal. The organ bath was perfused continuously with physiological solution of the following composition: NaCl 118 mM, KCl 3.5 mM, 4-(2-hydroxyethyl)-1-piperazineethanesulfonic acid (HEPES) 20 mM, $CaCl_2$ 1.5 mM, $MgCl_2$ 1 mM, D-Glucose 10 mM (adjusted to pH 7.4) and bubbled continuously with 100 % O_2. Bicarbonate buffering was not used. The bath was perfused with a peristaltic pump at a flow rate of 6-8 ml/min and the temperature of the solution entering the bath was maintained at 30-32°C with a Peltier block. The length of nerve between the stimulating and recording electrodes varied between 4–11 mm and the bath volume was 400 µl.

Pairs of chlorided silver wire were used to stimulate the nerve and record extracellular signals. For stimulation, a silver wire inside the glass pipette served as the anode and a second silver wire, in the organ bath, served as the cathode. Similarly, a silver wire inside the glass pipette and a second silver wire in the bath were used to record extracellular signals over the sealing resistance of the vaseline.

Extracellular sucrose gap recording

An organ bath with four compartments (see Fig. 2B) was constructed to record signals proportional to "average" axonal membrane potential. Compartments within the organ bath were separated from one another by silicone membranes through which the sural nerve was drawn to span all four compartments. The nerve was stimulated electrically with brief (1ms) pulses of constant current via silver wire electrodes inside the glass pipette (anode) and a

second wire in the extracellular bath. Extracellular signals were recorded using a silver wire in the extracellular bath and a second wire inside the compartment containing intracellular solution, i.e. across the sucrose "gap" compartment. The sucrose compartment was perfused continuously with sucrose solution (301 mosm) using a gravity feed system. The width of the sucrose gap varied between 2-3 mm with an aim to minimise the intra-axonal resistance. The extracellular compartment was perfused continuously with HEPES-buffered physiological solution (see above) warmed to 30-32°C. The intracellular compartment contained solution of the following composition NaCl 3.5 mM, KCl 118 mM, 4-(2-hydroxyethyl)-1-piperazineethanesulfonic acid (HEPES) 20 mM, $CaCl_2$ 1.5 mM, $MgCl_2$ 1 mM, D-Glucose 10 mM adjusted to pH 7.4.

Extracellular recording of the C-fibre compound action potential (CAP)

Signals were amplified (N104 Neurolog, Digitimer, Hertfordshire, UK), digitized (NI-600, National Instruments, USA) and processed on-line using QTRAC software (Prof. Hugh Bostock, Digitimer, Hertfordshire, UK). To isolate the C-fibre component of the electrically-evoked CAP (C-CAP) a digital window discriminator was implemented in QTRAC software (Fig. 1B, *grey lines*). The position of the time window was adjusted to be typically 5-20 ms after the electrical stimulus depending upon the length of nerve segment and the stimulus protocol. The C-CAP response to each electrical stimulus was analysed on-line, within this time window, to determine peak to peak amplitude and latency (Fig. 1B). Latency was taken as the time between stimulus onset and the first positive-crossing, within the window, of the C-CAP signal at an amplitude 50% of the maximum peak positive amplitude (Fig. 1B*, left trace horizontal line*).

For experiments using the sucrose gap technique, the same electrical stimulus parameters were used to generate the C-CAP. In addition, a DC-coupled amplifier was constructed to record extracellular signals across the sucrose gap (Fig. 2B). For analysis, DC potentials were determined by averaging the signal over a 200 ms window immediately prior to each electrical stimulus.

Determination of electrical excitability in C-fibre axons

We used threshold tracking to monitor the electrical excitability of C-fibre axons as described previously (Moalem *et al.*, 2005). C-fibre axonal excitability was determined using constant current stimuli (1ms duration) and the rate of electrical stimulation was typically 1 Hz. Electrical stimuli of different amplitude were delivered in a rolling sequence of three, i.e. 1,2,3,1,2,3… corresponding to the following conditions. Stimulus condition 1 was supra-

maximal, i.e., a stimulus delivered at a current intensity at least 3x threshold, typically 50 μA, and intended to excite all axons and thus evoke a maximal C-CAP. This supra-maximal stimulus intensity remained constant throughout the experiment and the response is termed the 100% C-CAP (100% insets, Fig. 2A). The intensity of the second stimulus in the sequence was adjusted each cycle by the software with the aim of evoking a C-CAP with an amplitude corresponding to 40% (40% insets, Fig. 2A) of the maximal (100%) C-CAP. The third stimulus was also adjusted by the QTRAC software to evoke a C-CAP of 40% amplitude (cond. 40%., Fig. 1B) but this was conditioned by a preceding supra-maximal electrical stimulus (100 μA) 30 msec earlier. For each set of three stimuli (1,2,3) the stimulus current required to evoke an unconditioned 40% C-CAP (stimulus 2) and a 40% C-CAP conditioned with a preceding pulse (stimulus 3) were used to calculate an excitability index.

$$Excitability\ index\ (\%) = 100 * \frac{(40\%\ cond.current - 40\%\ current)}{40\%\ current} \qquad \text{Equation 1}$$

Application of substances

Pharmacological agents were added to the solution perfusing the bath by switching the intake source of the peristaltic pump from one cylinder with extracellular HEPES solution to another containing the substance diluted in extracellular HEPES solution. The time required for the solution to reach the organ bath was approximately 35 sec and the shading indicating substance application in the figures have been adjusted for this delay such that the shading indicates the substance reaching the bath.

Induction and assessment of activity depending slowing (ADS)

In response to sustained (tens of seconds) low frequency (1-10 Hz) action potential activity, unmyelinated C-fibre axons exhibit a characteristic accommodative slowing of their axonal conduction speed, commonly referred to as activity dependent slowing (ADS). ADS was quantified as the relative change in latency of the C-CAP response during stimulation at 2.5 Hz. Using an electrical stimulation frequency of 0.5 Hz (every 2 sec), the frequency of stimulation was stepped to 2.5 Hz for a period of 3 minutes before returning to 0.5 Hz. Changes in axonal excitability during stimulation at 2.5 Hz together with the peak amplitude and latency of the C-fibre CAP were monitored. ADS was calculated during the period of 2.5 Hz stimulation by dividing the latency of each 100% C-CAP by the average latency of C-CAP responses to the 15 stimuli preceding stimulation at 2.5 Hz. ADS is an integrative measure affected by relative changes in axonal membrane potential (Bostock *et al.*, 2003), Na_V availability (De Col *et al.*, 2008) and intracellular ion concentrations (Bliss & Rosenberg, 1979).

Single fibre recordings from the isolated skin-saphenous nerve preparation

Adult mice were killed (see Anaesthesia and Housing) and a segment of hindpaw hairy skin removed by dissection together with its innervating saphenous nerve. The skin flap was pinned, corium side up, to the silicone base of an organ bath perfused continuously with physiological solution of the following composition 107.8mM NaCl, 26.2mM NaCO3, 9.64mM Na-gluconate, 7.6mM sucrose, 5.05mM glucose, 3.48mM KCl, 1.67mM NaH2PO4, 1.53 CaCl2mM and 0.69mM MgSO4 and bubbled with carbogen (95% oxygen and 5% carbon dioxide) to pH 7.4 and warmed to 32±1°C. The saphenous nerve was drawn through a vaseline seal into a chamber filled with paraffin oil. The nerve was teased apart gently into fine filaments. Filaments were draped over gold wire recording electrodes and extracellular signals filtered (3Hz-3kHz), amplified (N104 Neurolog, Digitimer, Hertfordshire, UK) and digitized (micro1401, CED, Cambridge, UK).

Functionally single A- and C-fibre axons were identified using a blunt glass rod to locate mechanical receptive fields in the skin flap. A tungsten wire positioned at the centre of the mechanical receptive field served as the cathode for electrical stimulation. Individual units were characterized by their responsiveness to thermal and mechanical stimuli. Mechanical activation threshold was determined with von Frey filaments (1-128mN). A filament load producing a response (i.e. 1 or more action potentials) in at least three of five presentations was deemed above threshold. For thermal stimuli and application of chemicals, an aluminium cylinder (9mm OD) placed around the cathode allowed local perfusion of the receptive field. For cooling stimuli, the volume within the ring was evacuated and replaced with cooled solution. A Peltier device heated the fluid entering the ring from 32°C to 46°C in 20s. Fibres were considered heat/cold responsive if at least two action potentials occurred during the heat ramp stimulus. Heat threshold was defined as the temperature of the solution at the time of initiation of the second spike after correction for axonal conduction. GABA was applied to the solution perfusing the aluminum ring.

RNA extraction and qRT-PCR.

RNA samples were extracted from acutely excised DRG using Trizol™ (Life Technologies Italia, Monza, Italy) according to the manufacturer's protocol. RNA was quantified with NanoDrop2000 (Thermo Fisher Scientific, Monza, Italy). Pure RNA was obtained after DNAse treatment with a kit from Sigma-Aldrich (Catalog Number AMPD1). A 1 µg quantity of RNA was reverse-transcribed to cDNA using iScript™ Reverse Transcription Supermix for qRT-PCR (Bio-Rad, Segrate, Milan, Italy). Primers were designed using

PrimerBlast (NIH, Bethesda, MD, USA). Primer sequences for $GABA_AR$ subunits and the housekeeping genes α-tubulin and 18s-rRNA are shown in Table 1. From each sample, 10 ng of cDNA was used for quantitative PCR. RT-qPCR was performed by measuring incorporation of EVA Green dye (Bio-Rad) with a CFX 96 Real Time System-C1000 touch thermal cycler (Bio-Rad). CFX Manager 2.0 software (Bio-Rad) was used for data analysis. The threshold cycle number (Ct) of both the calibration and samples of interest were normalized to the geometric mean of Ct for the two endogenous housekeeping genes. The Pfaffl method was used for analysis and results are expressed normalized to the mean level of housekeeping genes (Pfaffl, 2001). For calibration, we used RNA obtained from control samples.

Immunofluorescence (IFL)

Explanted sural and sciatic nerves were de-sheathed before being fixed in 4% paraformaldehyde (PFA, Sigma-Aldrich), cryopreserved using crescent % sucrose solution, embedded in OCT (Sakura, Leiden, The Netherlands) and cut in cross-section or longitudinal-section. Primary antibodies included: guinea pig anti $GABA_A$-R α2 1:250 (generous gift by Prof. Fritschy, Univ. of Zurich, Switzerland), mouse anti-Smi31 anti heavy neurofilament (H-NF) 1:500 (Biolegend, San Diego, CA, US). Secondary antibodies included: goat anti-guinea pig Alexa Fluor 488 1:500 (Abcam, Italy) and goat anti-mouse TRITC 1:500 (Sigma Aldrich, Italy). After washing, nerves were mounted using Vectashield™ (Vector Laboratories, Burlingame, CA, USA) and nuclei were stained with 4,6-diamidino-2-phenylindole (Dapi). To ensure specificity, control slides were incubated in solutions lacking primary antibodies. Confocal images were acquired with a Zeiss LSM 510 System (Zeiss, Göttingen, Germany) using a water immersion 40x objective (LD C-Apochromat 40x/1.1 W Korr UV VIS IR), pin hole set to 1 Airy unit and filters sets for FITC (ex 493, em 517, bp 400-550), TRITC (ex 553, em 568, bp 540-700) and DAPI (ex 353 em 465. bp 400-600) yielding an average Z-optical section of 250nm. Images were processed with Image Pro-Plus 6.0 (Media Cybernetics, Bethesda, MA, USA). IFL was repeated on negative samples to establish antibody reliability and specificity.

HPLC Determination of GABA in sural nerve

Sural nerves were desheathed and immersed individually for 15 minutes in physiological solution, during which time the nerve was either stimulated electrically (1 ms, 100 μA) at 0.5 Hz (plus 2 bouts at 2Hz for 3mins) or not. Quantification of GABA in the bathing solution was determined by high performance liquid chromatography (HPLC) (Alliance 2095 module

with remote control by the Empower 3 Software; Waters Italia s.p.a, Sesto San Giovanni, Italy) coupled to a fluorometric detection system (Shimadzu RF-10AXL; excitation 350 nm; emission 450 nm) as previously described (Milanese *et al.*, 2013). Eluates were processed without dilution and maintained at 4°C during the quantification procedure. The method consisted of pre-column derivatization of the sample with O-phthalaldehyde (Sigma-Aldrich, St. Louis, MO, USA) and gradient separation on a C18 reverse-phase chromatographic column (Agilent MicroSpher C18, S100x4.6, 3 μm; CPS Analitica, Milano, Italy) maintained at 30 °C. Homoserine was used as an internal standard (Sigma-Aldrich, St. Louis, MO, USA). The following gradient buffers were utilized: solvent A, 0.1 M sodium acetate (pH 5.8)/methanol 80:20; solvent B, 0.1 M sodium acetate (pH 5.8)/methanol, 20:80; solvent C, sodium acetate (pH 6.0)/methanol, 80:20. The total gradient HPLC program needs 25 min of elution for each sample.

Chemicals and solutions

GABA, 1(*S*),9(*R*)-(−)-bicuculline methiodide, muscimol, (±)-baclofen, gaboxadol/THIP (4,5,6,7-tetrahydroisoxazolo (5,4-**c**)pyridin-3(-ol)), bumetanide, NaCl, KCl, 4-(2-hydroxyethyl)-1-piperazineethanesulfonic acid (HEPES), $CaCl_2$, $MgCl_2$ and D-Glucose were from Sigma-Aldrich (Munich, Germany). Allopregnanolone (ALLO) was from Steraloids (Newport, RI, USA). Inflammatory soup comprised histamine (1 μM), bradykinin (5 μM), prostaglandin E2 (1 μM) and serotonin hydrochloride (1 μM), all from Sigma-Aldrich (Munich, Germany). Stock solutions were prepared in PBS for GABA (1M), bicuculline (10mM), muscimol (100mM), baclofen (100mm), histamine (1mM) and serotonin (1mM) . Ethanol was the solvent for stock solutions of allopregnanolone (10mM), gaboxadol (THIP, 100mM) and prostaglandin E2 (1mM). This resulted in final ethanol concentrations in the perfusing solution between 0.0001% and 0.1% and ethanol applied alone at 0.1% was without effect on C-fibre excitability parameters (n=4). The stock solution for bumetanide was dissolved in dimethyl sulfoxide (DMSO, 100mM). This resulted in a maximum dilution for DMSO of 0.02% and DMSO applied alone at 0.02% was without effect on C-fibre excitability parameters (n=8). For bradykinin, 1% acetic acid was the solvent for the 2mM stock solution. Acetic acid (1%) applied alone to sural nerve was without effect on excitability parameters (n=3). The procedure of diluting stock solution in physiological solution to the desired concentration was the same for all substances and was performed on the day of each experiment.

Data and statistical analysis

Electrophysiological data were analysed with custom routines in Igor Pro (Wavemetrics, Lake Oswego, OR, USA). Statistical tests were performed with GraphPad Prism 8.00 (San Diego, CA, USA). Kolmogorov-Smirnov and Shapiro-Wilk tests were used to assess the applicability of parametric statistical tests. The resulting Kolgomorov-Smirnov distance (D) or Shapiro-Wilk (W) statistic is reported in the legend to each Figure. Parametric comparisons between groups were made either with t-tests or repeated measures (RM)-ANOVA. Wilcoxon and Friedman tests were used for non-parametric group comparisons. Data are shown in Figures as individual values together with error bars indicating standard deviation. Values of p less than 0.05 were considered significant. 'n' values indicate the number of individual sural nerves.

Results

GABA increased electrical excitability in unmyelinated axons

We used threshold tracking techniques to examine the effect of GABA on the electrical excitability of unmyelinated C-fibre axons in isolated segments of mouse sural nerve (Fig. 1A&B). In response to GABA (100 μM) the current intensity required to maintain a 40% C-CAP (Fig. 1B, centre) decreased substantially (current trace; Fig. 1C & D) while the stimulus current required to maintain a conditioned 40% C-CAP (30ms after a pre-conditioning stimulus, Fig. 1B, right) fell only marginally (current trace; Fig. 1C&D). The reduction in stimulus current during GABA corresponds to an increase in axonal excitability and is quantified using an excitability index (Exc. index trace, Fig. 1C, Fig. 1E and Eq.1). The GABA evoked increase in excitability index was paralleled by a reduction in C-CAP latency (latency trace; Fig. 1C & F), that is, an increase in axonal conduction velocity. Both the increase in electrical excitability (Fig. 1E) and the increase in conduction speed (reduction in latency, Fig. 1F) are consistent with axonal depolarization. Notably, during application of GABA (200 μM), a reduction in the intensity of stimulus current required to evoke C-CAPs of all sizes is observed (Fig. 1G).

Axonal C-fibre responses to application of GABA over several minutes showed distinct kinetics, comprising an initial transient increase in excitability followed by a sustained plateau that was maintained for the duration of GABA application (Fig. 1H). We speculated that this kinetic profile of excitability change mirrored changes in $GABA_AR$ mediated current. The initial transient increase in excitability could reflect a transient inward current driven by an initially elevated intracellular chloride concentration that decreases rapidly due

to chloride efflux through $GABA_AR$ (Fig. 1H phase 1). The sustained component is interpreted as a steady-state $GABA_AR$ current carried by chloride and HCO_3^- efflux with the former sustained by NKCC1 mediated chloride influx (Fig. 1H phase 2; and schematic Fig. 5E).

GABA depolarised axons in mouse sural nerve

Previous reports indicate that GABA depolarised axons in the cervical vagus (Brown & Marsh, 1978; Jackson *et al.*, 1992). To confirm an effect of GABA on axonal membrane potential and determine its relation to the observed increase in electrical excitability (Fig. 1) we recorded electrically-evoked sural nerve C-CAPs and DC voltage using a sucrose gap system (Fig. 2B). Consistent with previous reports, GABA (300 μM) depolarised sural nerve axons by 0.61 ±0.17 mV (n=4, DC trace Fig. 2A&C). Depolarisation in response to GABA was observed together with an increase in the amplitude of the 40% C-CAP signal (Fig. 2A, 2nd row of insets 40% C-CAP and Peak lower trace). In response to GABA, axonal depolarisation preceded the increase in excitability. This lag in excitability increase relative to the increase in DC potential arises from the predictive calculation for stimulus current intensity for each ensuing stimulus by the QTRAC software. The magnitude of depolarisation of sural nerve axons was independent of C-CAP amplitude (Fig. 2D).

Exogenous GABA does not evoke action potentials in individual A or C-fibres

GABA has been shown to evoke action potential firing in approximately two thirds of cultured DRG neurons (Staley *et al.*, 1996). Given that GABA depolarised peripheral axons (Fig. 2) we tested whether GABA might also be able to evoke action potentials in cutaneous sensory axons. Recordings were made from 7 individual cutaneous A-fibres (c.v. 8.3±3.6 m/s) and 12 individual C-fibres (5xC-MH, 2xC-MHC, 4xC-HTM, 1xC-Mi; c.v. 0.45±0.04 m/s) in mouse saphenous nerve. Receptive fields were identified in the skin using a mechanical search stimulus and an electrode (cathode) placed at the centre of this field. Electrical stimulation at 0.125 Hz (every 8s) was used to determine conduction velocity and to monitor single axons during application of GABA (100-300 μM). GABA was applied to the solution perfusing an aluminium cylinder (1 cm diameter) positioned onto the skin and centred about the stimulus cathode. GABA (100-300 μM) was applied to the solution within the aluminium cylinder for 3 minutes. For 7 A-fibres or 12 C-fibre axons there was no discernible action potential activity during GABA application nor in the 5 minutes thereafter. GABA was also without effect on conduction latency in individual axons. The lack of effect of GABA on single fibre conduction velocity contrasts with the shortening of conduction

latency observed in sural nerve C-CAP recordings (Fig. 1F). This difference most likely arises from the aluminium ring used in the single fibre recordings that restricts exposure to GABA to a short length of terminal axon that represents not more than 10% of the conduction path. Thus, while GABA depolarised peripheral axons (Fig. 2), it did not evoke action potentials in cutaneous A- or C-fibres.

GABA induced increase in C-fibre excitability is mediated by $GABA_AR$

GABA (1-1000 μM) increased electrical excitability in sural nerve C-fibres and this effect was mediated by $GABA_AR$. GABA-evoked excitability increases were blocked by the competitive $GABA_AR$ antagonist bicuculline (50 μM, Fig. 3A&B) and mimicked by the $GABA_AR$ agonists muscimol (100 μM, Fig. 3C&D) and THIP (Gaboxadol, 100-200μM, Fig 4F). In addition, ALLO (1 μM), a positive allosteric modulator of $GABA_AR$, potentiated the increase in C-fibre excitability in response to GABA (Fig. 3F&G). Recent evidence has indicated that $GABA_BR$ activation can ameliorate inflammatory sensitization of C-fibres (Hanack *et al.*, 2015). Despite this, the $GABA_BR$ agonist baclofen (100 μM) had no discernible effect on C-fibre excitability, axonal conduction velocity or C-CAP amplitude (Fig. 3C&E). These results demonstrate that the concentration dependent increase in C-fibre excitability observed in response to GABA (Fig. 3H; EC_{50} of 31.28±18.88 μM; n= 61) is mediated by activation of axonal $GABA_AR$.

β3 is required for functional $GABA_AR$ in peripheral C-fibres

In sural nerves from mice conditionally lacking β3-$GABA_A$ in most DRG neurons (*Adv;β3*) or selectively in NaV1.8-expressing nociceptive neurons (*sns;β3),* GABA (up to 1 mM) produced no discernible effect on C-fibre excitability (Fig. 4A-D), conduction latency or C-CAP amplitude. This consolidated $GABA_AR$ as the mediator of GABA evoked excitability changes in C-fibre axons and highlighted the obligatory role of β3 in the formation of functional axonal $GABA_AR$.

RT-qPCR was used to quantify mRNA for nine $GABA_AR$ subunits, including α2-5, β1-3, δ and γ2 in explants of whole lumbar DRG (Fig. 4E). β3, α2 and γ2 were the most abundant $GABA_AR$ subunit transcripts and these are typically associated with synaptic $GABA_AR$. mRNA levels for β1 were lower than previously reported in cultured DRG neurons (Faroni *et al.*, 2019). The δ subunit is characteristic of high affinity extra-synaptic $GABA_AR$ and its expression was only marginally above the detection limit (Fig. 4E). Consistent with low mRNA levels for the δ subunit (Fig. 4E) concentrations of THIP (gaboxadol) below 1 μM, at which it is a selective δ-subunit agonist (Meera *et al.*, 2011), did not affect axonal excitability

(Fig. 4F). However, THIP did increase C-fibre excitability at concentrations above 10 μM, at which it is a non-selective $GABA_AR$ agonist.

The presence of α2 mRNA in DRG explants was confirmed by immunostaining sural (Fig. 4G) and sciatic (Fig. 4H) nerve from WT mice. Fluorescence signal for α2 was observed in some myelinated axons, co-stained with heavy neurofilament as well as in some unmyelinated axons, not associated with heavy neurofilament (Fig 4G&H).

NKCC1 determines the size of the GABA evoked increase in axonal excitability

To examine the role of intracellular chloride in determining the amplitude of GABA-induced changes in C-fibre excitability, bumetanide (20 μM) was used to block NKCC1 inward Cl^- transport. Under control conditions, successive application of GABA (300 μM) at 10 min intervals elicited robust and stereotyped increases in axonal excitability (Fig. 5A, upper trace). Blockade of NKCC1 with bumetanide (20 μM) reduced progressively the amplitude of successive axonal responses to GABA (300 μM, central trace) and also resulted in a protracted increase in baseline excitability (Fig. 5A, lower trace). The reduction in axonal GABA response amplitude in the presence of bumetanide (Fig. 5B) is likely to result from an inability of NKCC1 to re-establish the intra-axonal chloride concentration following each GABA application. The slow increase in axonal excitability over 10-20 min in the presence of bumetanide (Fig. 5A&B) is interpreted as reflecting a slow membrane depolarisation. This could arise through a reduction in inward K^+ transport during bumetanide reducing E_K and progressively depolarizing axons.

$GABA_AR$ mediated chloride currents are sufficient to alter intra-cellular chloride concentration in neuronal somata (Ballanyi & Grafe, 1985) and this is exacerbated in small volume structures such as the dendrites of CA1 pyramidal neurons (Staley & Proctor, 1999) and presumably small diameter unmyelinated axons. To examine this possibility in C-fibres, GABA (300 μM) was applied initially for 2 minutes. Subsequently, 5 s GABA applications were made every 2 minutes (Fig. 5C) to determine the rate of recovery of axonal GABA responses. The first 7 responses to 5s GABA applications showed a progressive reduction in the transient response (Fig. 5C, grey shading) consistent with depletion of intra-axonal chloride. Notably, the transient GABA response amplitude decreased to a value corresponding to the amplitude of the initial sustained response to GABA (Fig. 5C, grey shading). The interval between successive 5s GABA applications was then lengthened, from 2 out to 6 minutes (Fig. 5C, lightest grey shading) during which the transient response to GABA increased as the recovery interval was lengthened. The inflection point for a Sigmoid

fit to the recovery profile was 4.88±0.42 minutes (Fig. 5D, n=17) with a time constant of 1.053±0.484 minutes. This recovery is indicative of the rate at which the chloride gradient was restored.

Previous reports indicate that phosphorylation of NKCC1 by inflammatory mediators is associated with an elevated intracellular Cl^- concentration in isolated DRG neurons (Funk *et al.*, 2008). To examine whether this is applicable to axons, sural nerves were exposed to inflammatory soup (Steen *et al.*, 1992) comprising histamine (1 mM), bradykinin (2 mM), prostaglandin E_2 (PGE_2; 100 μM) and serotonin (1 mM) for 10-30 minutes. This led to a prominent increase in the amplitude of axonal excitability responses to GABA (100 μM) (Fig. 5F&G) consistent with an elevated E_{Cl} associated with increased NKCC1 activity.

Action potential firing stimulates NKCC1 mediated axonal chloride loading

In immature CA1 pyramidal neurons, the thermodynamic set point of NKCC1 activity increased in proportion to action potential firing rate (Brumback & Staley, 2008) and there has been speculation that a similar process may occur in somatosensory C-fibres (Price *et al.*, 2009). To examine the role of action potential firing in modulating NKCC1 activity in C-fibre axons, axonal GABA (100 μM) responses were first determined at different rates of electrical stimulation from 0.5 to 1.7 Hz (Fig. 6A). Consistent with previous reports (Carr *et al.*, 2010), axonal GABA response amplitude increased in proportion to the prevailing rate of electrical stimulation (Fig. 6A&B). Importantly, in the period following high frequency stimulation the increase in GABA response amplitude persisted for several tens of minutes (Fig. 6A, 6E). An activity dependent loading of axons with chloride could account for this. To test this idea, repeat bouts of 2.5 Hz electrical activity were applied at 10 min intervals and a progressive increase in GABA response amplitude was evident (Fig. 6C). This increase in amplitude was apparent both for the transient and sustained components of GABA responses (Fig. 6D). In addition, the potentiation of GABA responses by bouts of 2.5Hz electrical stimulation was long-lasting and persisted for up to 30 minutes (Fig. 6E&F). To exclude a possible shift in affinity of $GABA_AR$, repeat applications of GABA (300 μM) at a constant low stimulus rate (1 Hz) were applied without intervening activity bouts and this had no effect on axonal GABA response amplitude (Fig. 6G&H). To further exclude changes in $GABA_AR$ affinity, $GABA_AR$ was blocked with bicuculline during bouts of activity at 2.5 Hz and this did not prevent the enhancement of axonal GABA responses (Fig. 6I&J).

In a second step, we blocked NKCC1 with bumetanide (20 μM) during the period of 2.5 Hz electrical stimulation and this significantly hampered the ability of action potential activity to

enhance axonal GABA responses (Fig. 6K&L). This demonstrates that elevated NKCC1 activity is coupled to increased action potential firing in C-fibre axons.

$GABA_A$ activation limits activity-dependent slowing in C-fibres

Having established a link between action potential activity and NKCC1 mediated axonal chloride loading (Fig. 6K&L) we examined the effect of intra-axonal chloride manipulations on C-fibre excitability during sustained low frequency challenge. During sustained low frequency stimulation, eg. 2.5 Hz for 3 min, C-fibres show a progressive slowing of their axonal conduction velocity, activity-dependent slowing (ADS; Fig. 7A, black trace). ADS was enhanced in nerves from mice conditionally lacking $GABA_AR$ (*sns;*$\beta 3^{-/-}$; Fig. 7A&B). ADS was also enhanced by $GABA_AR$ blockade with bicuculline (50 μM; Fig. 7C&D). In contrast, ADS was reduced by GABA (1 mM, Fig. 7A&B) and the positive $GABA_AR$ allosteric modulator ALLO (1 μM; Fig. 7E&F). This indicates that $GABA_AR$ activation limits the extent of ADS. However, when NKCC1 was blocked with bumetanide (20 μM) ADS was enhanced (Fig. 7G&H) further supporting the idea that NKKC1 mediated axonal chloride loading is coupled to action potential firing. We conclude that NKCC1 maintains and possibly elevates intra-axonal chloride during action potential firing in C-fibres. This feed-forward chloride loading allows activation of a chloride conductance, eg. $GABA_AR$, to stabilise axonal excitability and thus limit ADS.

GABA in sural nerve

The possibility of endogenous regulation of C-fibre excitability via axonal $GABA_A$ prompted us to examine levels of endogenous GABA in sural nerve. Desheathed sural nerve segments were bathed in physiological solution for 15 minutes and HPLC revealed nanomolar concentrations of GABA (12.16±0.81 nM; Fig. 8B&E) in the bathing solution. Interestingly, the concentration of GABA was not significantly altered when the nerve was stimulated electrically (at 0.5Hz throughout with two bouts at 2.5 Hz each for 3 minutes) during the 15 minute bathing period (Fig. 8C&F and 8G). This suggests that axonal action potential activity may not be associated with an increase in endogenous GABA in peripheral nerve.

DISCUSSION

We confirm the presence of functional $GABA_AR$ along peripheral unmyelinated axons. Activation of axonal $GABA_AR$ depolarized axons in sural nerve and increased the electrical excitability of C-fibre axons. Notably, GABA-evoked increases in axonal excitability were dependent upon the previous firing history of axons with higher firing rates resulting in increased excitability responses to GABA. NKCC1 was responsible for this coupling of action potential firing to GABA-evoked excitability response size. This suggests that NKCC1 regulates intra-axonal chloride in proportion to action potential load. We used GABA to probe the effect of opening a chloride conductance during sustained firing. GABA reduced the extent of ADS during 2.5 Hz challenge, while NKCC1 blockade, $GABA_AR$ blockade and deletion (sns^{Cre};$gabrb3^{fl/fl}$) all exacerbated ADS (Fig. 7). This demonstrates that chloride channel opening stabilised C-fibre excitability during activity. We posit that the coupling of NKCC1 to action potential firing rate acts in a feed-forward manner to maintain an elevated intra-axonal chloride concentration in C-fibres. The resulting elevated chloride concentration allows an axonal chloride conductance, possibly $GABA_AR$, to stabilise excitability during sustained firing.

Sustained action potential activity in unmyelinated axons leads to a reduction in their axonal conduction velocity and their excitability that is attributed to a combination of activity-dependent hyperpolarization (Rang & Ritchie, 1968), accumulation of intracellular Na^+ (Bliss & Rosenberg, 1979) and inactivation of Na_V channels (De Col *et al.*, 2008; Tigerholm *et al.*, 2015). CA1 pyramidal neurones maintain an elevated intracellular chloride concentration during trains of action potentials through a shift in the thermodynamic equilibrium set point for NKCC1 (Brumback & Staley, 2008). While elevated intra-axonal chloride is a pre-requisite for the modulation of excitability, a chloride conductance is required to affect membrane excitability. In hippocampal granule cells $GABA_AR$ can serve as a chloride conductance that is able to both reduce the fidelity of action potential conduction along unmyelinated mossy fibres at low intracellular chloride concentration and to enhance axonal excitability when chloride was elevated (Ruiz *et al.*, 2003). In addition, axonal conduction fidelity was increased following application of neuroactive steroids suggesting that $GABA_AR$ was basally active (Ruiz *et al.*, 2010). Similarly, GABA acting via axonal $GABA_AR$ increased excitability (Pugh & Jahr, 2011) and conduction fidelity (Dellal *et al.*, 2012) in the parallel fibres of cerebellar granule cells. In the case of somatosensory axons, excitability loss during sustained activity was enhanced by bicuculline (Fig. 7C) and reduced by

allopregnanolone (Fig. 7E) implying that both were able to modulate a basally activated $GABA_AR$.

There a remarkably few recognised sources of GABA in peripheral nerve. Schwann cells can synthesize both GABA and the neuroactive steroid allopregnanolone (Bonalume *et al.*, 2020; Colciago *et al.*, 2020). It has also been suggested that sensory axons themselves may be a source of GABA (Hanack *et al.*, 2015). Estimates of ambient GABA concentration in CSF range from mid-nanomolar to a few micromolar (Lerma *et al.*, 1986; Tossman *et al.*, 1986; Kennedy *et al.*, 2002) and here we detected low nanomolar concentrations of GABA in solution bathing sural nerve (Fig. 8). While it is possible that the local GABA concentration is elevated within peripheral nerve, especially in the restricted volume between glia and axons, only $GABA_ARs$ comprising the high-affinity δ subunit respond to GABA in the nanomolar range and the high-affinity δ subunit was conspicuously absent in DRG tissue (Fig. 4E) and C-fibre axons (Fig. 4F). Instead, synaptic α2, β3 and γ2 subunits predominated (Fig. 4E) and this is consistent with previous RT-PCR (Maddox *et al.*, 2004), *in-situ* hybridization (Ma *et al.*, 1993) and immunohistochemical findings (Lorenzo *et al.*, 2014). Although α2β2/3γ2 has typically been considered a constellation for synaptic $GABA_AR$ (Sassoe-Pognetto *et al.*, 2011) our results suggest its presence asynaptically, along peripheral axons. $GABA_ARs$ are spatially labile and thus able to diffuse between synaptic and extrasynaptic locations (Thomas *et al.*, 2005; Bogdanov *et al.*, 2006; Bannai *et al.*, 2009; Hannan *et al.*, 2019). In this context it is interesting that DRG neurons express low levels of gephyrin (Lorenzo *et al.*, 2014), a protein targeting $GABA_ARs$ to the post-synaptic domain (Tretter *et al.*, 2008).

Conditional deletion of the $GABA_AR$ β3 subunit ($sns^{Cre};\beta3^{-/-}$) abolished C-fibre excitability responses to GABA and this is consistent with reports indicating that β3 is required for GABAergic pre-synaptic inhibition in the spinal dorsal horn (Chen *et al.*, 2014; Zimmerman *et al.*, 2019). The complete abolition of axonal GABA responses in β3 nulls observed here (Fig. 4A-D) contrasts however with the incomplete reduction of GABA currents in the soma of DRG neurons from β3 nulls (Chen *et al.*, 2014). Residual GABA currents in β3 null DRG neurons may well be affected by expression changes associated with culturing, during which $GABA_AR$ is upregulated (Lee *et al.*, 2012).

$GABA_AR$ currents exhibit phasic and tonic kinetics often associated with synaptic and extra-synaptic $GABA_AR$ respectively and with time courses in the order of tens of milliseconds (Farrant & Nusser, 2005; Belelli *et al.*, 2017). Distinct from these kinetics, the transient and

sustained components of axonal excitability responses to GABA occurred over several tens of seconds (Fig. 1H). We interpret the initial transient component of axonal GABA responses as reflecting partial or complete collapse of the transmembrane chloride gradient. During prolonged GABA application in frog DRG neurons the chloride gradient can fall by 10-15 mV (Akaike *et al.*, 1987) and shifts in E_{Cl-} are likely to be amplified in peripheral axons that have low volumes and are exposed to GABA over a considerable (5-8 mm) length. In addition, $GABA_AR$ desensitization which exhibits time constants extending to tens of seconds depending upon the isoform (Bianchi & Macdonald, 2002; Gielen *et al.*, 2012), may also contribute to the transient component of axonal excitability responses to GABA. The sustained component of axonal GABA responses persisted for several minutes in the continued presence of GABA (Fig. 1H) and we interpret this to reflect sustained axonal depolarization. During prolonged GABA application an inward $GABA_AR$ current could be mediated by HCO3- with a contribution from chloride provided by NKCC1 mediated influx. Consistent with this, a reduction in the amplitude of sustained GABA responses was observed during NKCC1 blockade with bumetanide (Fig. 5A). We attribute the effect of bumetanide to its action on NKCC1 and not due to it acting as a non-competitive antagonist at $GABA_AR$ (Inomata *et al.*, 1988; Sung *et al.*, 2000) because it was possible to elicit prominent axonal GABA responses during bumetanide (Fig. 5A&B).

Here we posit that during ongoing action potential firing in peripheral C-fibres, axonal excitability is stabilised by NKCC1 maintenance of an elevated intra-axonal chloride concentration and a chloride conductance, eg. $GABA_AR$ (Fig. 9). We demonstrate that a pre-requisite for this effect is the coupling of NKCC1 activity to action potential load in order to maintain the intra-axonal chloride concentration. In unmyelinated axons, activation of $GABA_AR$ can utilise the chloride gradient to limit activity-dependent conduction slowing. Regulation of axonal chloride through manipulation of NKKC1 and chloride channel activation via $GABA_AR$ may be effective means to curtail firing in peripheral C-fibres locally at site associated with pain and itch.

ACKNOWLEDGEMENTS:

We are grateful to Prof. Jean-Marc Fritschy, University of Zurich, Switzerland, for $GABA_AR$ antibodies. We thank Mrs. Ballabio Marinella (University of Milan) and Anja Bistron (Heidelberg University) for helpful technical assistance. The study was supported by grants from MIUR (Progetto Eccellenza) and from University of Milan (PSR2019_VMAGN) to VM and the German Research Society (DFG) to MS (SFB1158/2-TP01), JH (SFB1158/1-Z01) and RWC (SFB1158/2-TP04) and a Short Term Grant 2017 (57314023) to VB.

AUTHOR CONTRIBUTIONs

VB performed all threshold tracking experiments. LFC and LC performed RT-qPCR for $GABA_A$-R subunits. AF and FF performed IFL studies. Sucrose gap and single fibre recordings were made by RD, RC, KS and TH. SL and JH generated conditional mice. MM and GB performed HPLC analysis. The study was designed by RC, MS, VB and VM. The manuscript was written by RC, VB, FF, MS, and VM.

COMPETING FINANCIAL INTEREST

The authors declare no competing financial interest.

ADDITIONAL INFORMATION

Data Availability Statement: The data that supports the findings of this study are available from either of the corresponding authors (VM or RC) upon reasonable request.

References

Agarwal N, Offermanns S & Kuner R. (2004). Conditional gene deletion in primary nociceptive neurons of trigeminal ganglia and dorsal root ganglia. *Genesis* **38,** 122-129.

Akaike N, Maruyama T, Sikdar SK & Yasui S. (1987). Sodium-dependent suppression of gamma-aminobutyric-acid-gated chloride currents in internally perfused frog sensory neurones. *J Physiol* **392,** 543-562.

Alvarez-Leefmans FJ, Gamino SM, Giraldez F & Nogueron I. (1988). Intracellular chloride regulation in amphibian dorsal root ganglion neurones studied with ion-selective microelectrodes. *J Physiol* **406,** 225-246.

Ballanyi K & Grafe P. (1985). An intracellular analysis of gamma-aminobutyric-acid-associated ion movements in rat sympathetic neurones. *J Physiol* **365,** 41-58.

Bannai H, Levi S, Schweizer C, Inoue T, Launey T, Racine V, Sibarita JB, Mikoshiba K & Triller A. (2009). Activity-dependent tuning of inhibitory neurotransmission based on GABAAR diffusion dynamics. *Neuron* **62,** 670-682.

Bardoni R, Takazawa T, Tong CK, Choudhury P, Scherrer G & Macdermott AB. (2013). Pre- and postsynaptic inhibitory control in the spinal cord dorsal horn. *Ann N Y Acad Sci* **1279,** 90-96.

Belelli D, Brown AR, Mitchell SJ, Gunn BG, Herd MB, Phillips G, Seifi M, Swinny JD & Lambert JJ. (2017). Endogenous neurosteroids influence synaptic GABAA receptors during post-natal development. *J Neuroendocrinol*.

Ben-Ari Y. (2002). Excitatory actions of gaba during development: the nature of the nurture. *Nat Rev Neurosci* **3,** 728-739.

Bhisitkul RB, Villa JE & Kocsis JD. (1987). Axonal GABA receptors are selectively present on normal and regenerated sensory fibers in rat peripheral nerve. *Exp Brain Res* **66,** 659-663.

Bianchi MT & Macdonald RL. (2002). Slow phases of GABA(A) receptor desensitization: structural determinants and possible relevance for synaptic function. *J Physiol* **544,** 3-18.

Bliss TV & Rosenberg ME. (1979). Activity-dependent changes in conduction velocity in the olfactory nerve of the tortoise. *Pflugers Arch* **381,** 209-216.

Bogdanov Y, Michels G, Armstrong-Gold C, Haydon PG, Lindstrom J, Pangalos M & Moss SJ. (2006). Synaptic GABAA receptors are directly recruited from their extrasynaptic counterparts. *EMBO J* **25,** 4381-4389.

Bonalume V, Caffino L, Castelnovo LF, Faroni A, Giavarini F, Liu S, Caruso D, Schmelz M, Fumagalli F, Carr RW & Magnaghi V. (2020). Schwann Cell Autocrine and Paracrine Regulatory Mechanisms, Mediated by Allopregnanolone and BDNF, Modulate PKCepsilon in Peripheral Sensory Neurons. *Cells* **9**.

Bostock H, Campero M, Serra J & Ochoa J. (2003). Velocity recovery cycles of C fibres innervating human skin. *J Physiol* **553,** 649-663.

Brown DA & Marsh S. (1978). Axonal GABA-receptors in mammalian peripheral nerve trunks. *Brain Res* **156,** 187-191.

Brumback AC & Staley KJ. (2008). Thermodynamic regulation of NKCC1-mediated Cl- cotransport underlies plasticity of GABA(A) signaling in neonatal neurons. *J Neurosci* **28,** 1301-1312.

Carr RW, Sittl R, Fleckenstein J & Grafe P. (2010). GABA increases electrical excitability in a subset of human unmyelinated peripheral axons. *PLoS One* **5,** e8780.

Chen JT, Guo D, Campanelli D, Frattini F, Mayer F, Zhou L, Kuner R, Heppenstall PA, Knipper M & Hu J. (2014). Presynaptic GABAergic inhibition regulated by BDNF contributes to neuropathic pain induction. *Nat Commun* **5,** 5331.

Colciago A, Bonalume V, Melfi V & Magnaghi V. (2020). Genomic and Non-genomic Action of Neurosteroids in the Peripheral Nervous System. *Front Neurosci* **14,** 796.

De Col R, Messlinger K & Carr RW. (2008). Conduction velocity is regulated by sodium channel inactivation in unmyelinated axons innervating the rat cranial meninges. *J Physiol* **586,** 1089-1103.

Dellal SS, Luo R & Otis TS. (2012). GABAA receptors increase excitability and conduction velocity of cerebellar parallel fiber axons. *J Neurophysiol* **107,** 2958-2970.

Du X, Hao H, Yang Y, Huang S, Wang C, Gigout S, Ramli R, Li X, Jaworska E, Edwards I, Deuchars J, Yanagawa Y, Qi J, Guan B, Jaffe DB, Zhang H & Gamper N. (2017). Local GABAergic signaling within sensory ganglia controls peripheral nociceptive transmission. *J Clin Invest* **127,** 1741-1756.

Faroni A, Melfi S, Castelnovo LF, Bonalume V, Colleoni D, Magni P, Arauzo-Bravo MJ, Reinbold R & Magnaghi V. (2019). GABA-B1 Receptor-Null Schwann Cells Exhibit Compromised In Vitro Myelination. *Mol Neurobiol* **56,** 1461-1474.

Farrant M & Nusser Z. (2005). Variations on an inhibitory theme: phasic and tonic activation of GABA(A) receptors. *Nat Rev Neurosci* **6,** 215-229.

Funk K, Woitecki A, Franjic-Wurtz C, Gensch T, Mohrlen F & Frings S. (2008). Modulation of chloride homeostasis by inflammatory mediators in dorsal root ganglion neurons. *Mol Pain* **4,** 32.

Gao XB & van den Pol AN. (2001). GABA, not glutamate, a primary transmitter driving action potentials in developing hypothalamic neurons. *J Neurophysiol* **85,** 425-434.

Gielen MC, Lumb MJ & Smart TG. (2012). Benzodiazepines modulate GABAA receptors by regulating the preactivation step after GABA binding. *J Neurosci* **32,** 5707-5715.

Gilbert D, Franjic-Wurtz C, Funk K, Gensch T, Frings S & Mohrlen F. (2007). Differential maturation of chloride homeostasis in primary afferent neurons of the somatosensory system. *Int J Dev Neurosci* **25,** 479-489.

Grundy D. (2015). Principles and standards for reporting animal experiments in The Journal of Physiology and Experimental Physiology. *Journal of Physiology-London* **593,** 2547-2549.

Hanack C, Moroni M, Lima WC, Wende H, Kirchner M, Adelfinger L, Schrenk-Siemens K, Tappe-Theodor A, Wetzel C, Kuich PH, Gassmann M, Roggenkamp D, Bettler B, Lewin GR, Selbach M & Siemens J. (2015). GABA blocks pathological but not acute TRPV1 pain signals. *Cell* **160,** 759-770.

Hannan S, Minere M, Harris J, Izquierdo P, Thomas P, Tench B & Smart TG. (2019). GABAAR isoform and subunit structural motifs determine synaptic and extrasynaptic receptor localisation. *Neuropharmacology*, 107540.

Inomata N, Ishihara T & Akaike N. (1988). Effects of diuretics on GABA-gated chloride current in frog isolated sensory neurones. *Br J Pharmacol* **93,** 679-683.

Jackson DM, Pollard CE & Roberts SM. (1992). The effect of nedocromil sodium on the isolated rabbit vagus nerve. *Eur J Pharmacol* **221,** 175-177.

Kaneko H, Putzier I, Frings S, Kaupp UB & Gensch T. (2004). Chloride accumulation in mammalian olfactory sensory neurons. *J Neurosci* **24,** 7931-7938.

Kaneko HP, I; Frings, S.; Gensch, T. (2002). Determination of Intracellular Chloride Concentration in Dorsal Root Ganglion Neurons by Fluorescence Lifetime Imaging. In *Calcium-Activated Chloride Channels*, ed. Fuller CM, pp. 167-189.

Kennedy RT, Thompson JE & Vickroy TW. (2002). In vivo monitoring of amino acids by direct sampling of brain extracellular fluid at ultralow flow rates and capillary electrophoresis. *J Neurosci Methods* **114,** 39-49.

Lee KY, Charbonnet M & Gold MS. (2012). Upregulation of high-affinity GABA(A) receptors in cultured rat dorsal root ganglion neurons. *Neuroscience* **208,** 133-142.

Lerma J, Herranz AS, Herreras O, Abraira V & Martin del Rio R. (1986). In vivo determination of extracellular concentration of amino acids in the rat hippocampus. A method based on brain dialysis and computerized analysis. *Brain Res* **384,** 145-155.

Lorenzo LE, Godin AG, Wang F, St-Louis M, Carbonetto S, Wiseman PW, Ribeiro-da-Silva A & De Koninck Y. (2014). Gephyrin clusters are absent from small diameter primary afferent terminals despite the presence of GABA(A) receptors. *J Neurosci* **34,** 8300-8317.

Lu J, Karadsheh M & Delpire E. (1999). Developmental regulation of the neuronal-specific isoform of K-Cl cotransporter KCC2 in postnatal rat brains. *J Neurobiol* **39,** 558-568.

Ma W, Saunders PA, Somogyi R, Poulter MO & Barker JL. (1993). Ontogeny of GABAA receptor subunit mRNAs in rat spinal cord and dorsal root ganglia. *J Comp Neurol* **338,** 337-359.

Maddox FN, Valeyev AY, Poth K, Holohean AM, Wood PM, Davidoff RA, Hackman JC & Luetje CW. (2004). GABAA receptor subunit mRNA expression in cultured embryonic and adult human dorsal root ganglion neurons. *Brain Res Dev Brain Res* **149,** 143-151.

Meera P, Wallner M & Otis TS. (2011). Molecular basis for the high THIP/gaboxadol sensitivity of extrasynaptic GABA(A) receptors. *J Neurophysiol* **106,** 2057-2064.

Milanese M, Tardito D, Musazzi L, Treccani G, Mallei A, Bonifacino T, Gabriel C, Mocaer E, Racagni G, Popoli M & Bonanno G. (2013). Chronic treatment with agomelatine or venlafaxine reduces depolarization-evoked glutamate release from hippocampal synaptosomes. *BMC Neurosci* **14,** 75.

Mitchell EA, Herd MB, Gunn BG, Lambert JJ & Belelli D. (2008). Neurosteroid modulation of GABAA receptors: molecular determinants and significance in health and disease. *NeurochemInt* **52,** 588-595.

Moalem G, Grafe P & Tracey DJ. (2005). Chemical mediators enhance the excitability of unmyelinated sensory axons in normal and injured peripheral nerve of the rat. *Neuroscience* **134,** 1399-1411.

Orefice LL, Zimmerman AL, Chirila AM, Sleboda SJ, Head JP & Ginty DD. (2016). Peripheral Mechanosensory Neuron Dysfunction Underlies Tactile and Behavioral Deficits in Mouse Models of ASDs. *Cell* **166,** 299-313.

Pfaffl MW. (2001). A new mathematical model for relative quantification in real-time RT-PCR. *Nucleic Acids Res* **29,** e45.

Price TJ, Cervero F, Gold MS, Hammond DL & Prescott SA. (2009). Chloride regulation in the pain pathway. *Brain Res Rev* **60,** 149-170.

Pugh JR & Jahr CE. (2011). Axonal GABAA receptors increase cerebellar granule cell excitability and synaptic activity. *J Neurosci* **31,** 565-574.

Rang HP & Ritchie JM. (1968). On the electrogenic sodium pump in mammalian non-myelinated nerve fibres and its activation by various external cations. *J Physiol* **196,** 183-221.

Rivera C, Voipio J & Kaila K. (2005). Two developmental switches in GABAergic signalling: the K+-Cl- cotransporter KCC2 and carbonic anhydrase CAVII. *J Physiol* **562,** 27-36.

Rudomin P & Schmidt RF. (1999). Presynaptic inhibition in the vertebrate spinal cord revisited. *Exp Brain Res* **129,** 1-37.

Ruiz A, Campanac E, Scott RS, Rusakov DA & Kullmann DM. (2010). Presynaptic GABAA receptors enhance transmission and LTP induction at hippocampal mossy fiber synapses. *Nat Neurosci* **13,** 431-438.

Ruiz A, Fabian-Fine R, Scott R, Walker MC, Rusakov DA & Kullmann DM. (2003). GABAA receptors at hippocampal mossy fibers. *Neuron* **39,** 961-973.

Sassoe-Pognetto M, Frola E, Pregno G, Briatore F & Patrizi A. (2011). Understanding the molecular diversity of GABAergic synapses. *Front Cell Neurosci* **5,** 4.

Schobel N, Radtke D, Lubbert M, Gisselmann G, Lehmann R, Cichy A, Schreiner BS, Altmuller J, Spector AC, Spehr J, Hatt H & Wetzel CH. (2012). Trigeminal ganglion neurons of mice show intracellular chloride accumulation and chloride-dependent amplification of capsaicin-induced responses. *PLoS One* **7,** e48005.

Staley K, Smith R, Schaack J, Wilcox C & Jentsch TJ. (1996). Alteration of GABAA receptor function following gene transfer of the CLC-2 chloride channel. *Neuron* **17,** 543-551.

Staley KJ & Proctor WR. (1999). Modulation of mammalian dendritic GABA(A) receptor function by the kinetics of Cl- and HCO3- transport. *J Physiol* **519 Pt 3,** 693-712.

Steen KH, Reeh PW, Anton F & Handwerker HO. (1992). Protons selectively induce lasting excitation and sensitization to mechanical stimulation of nociceptors in rat skin, in vitro. *J Neurosci* **12,** 86-95.

Sung KW, Kirby M, McDonald MP, Lovinger DM & Delpire E. (2000). Abnormal GABAA receptor-mediated currents in dorsal root ganglion neurons isolated from Na-K-2Cl cotransporter null mice. *J Neurosci* **20,** 7531-7538.

Thomas P, Mortensen M, Hosie AM & Smart TG. (2005). Dynamic mobility of functional GABAA receptors at inhibitory synapses. *Nat Neurosci* **8,** 889-897.

Tigerholm J, Petersson ME, Obreja O, Eberhardt E, Namer B, Weidner C, Lampert A, Carr RW, Schmelz M & Fransen E. (2015). C-fiber recovery cycle supernormality depends on ion concentration and ion channel permeability. *Biophys J* **108,** 1057-1071.

Tossman U, Jonsson G & Ungerstedt U. (1986). Regional distribution and extracellular levels of amino acids in rat central nervous system. *Acta Physiol Scand* **127,** 533-545.

Toyoda H, Yamada J, Ueno S, Okabe A, Kato H, Sato K, Hashimoto K & Fukuda A. (2005). Differential functional expression of cation-Cl- cotransporter mRNAs (KCC1, KCC2, and NKCC1) in rat trigeminal nervous system. *Brain Res Mol Brain Res* **133,** 12-18.

Tretter V, Jacob TC, Mukherjee J, Fritschy JM, Pangalos MN & Moss SJ. (2008). The clustering of GABA(A) receptor subtypes at inhibitory synapses is facilitated via the direct binding of receptor alpha 2 subunits to gephyrin. *J Neurosci* **28,** 1356-1365.

Zeilhofer HU, Wildner H & Yevenes GE. (2012). Fast synaptic inhibition in spinal sensory processing and pain control. *Physiol Rev* **92,** 193-235.

Zhang XL, Lee KY, Priest BT, Belfer I & Gold MS. (2015). Inflammatory mediator-induced modulation of GABAA currents in human sensory neurons. *Neuroscience* **310,** 401-409.

Zimmerman AL, Kovatsis EM, Pozsgai RY, Tasnim A, Zhang Q & Ginty DD. (2019). Distinct Modes of Presynaptic Inhibition of Cutaneous Afferents and Their Functions in Behavior. *Neuron* **102,** 420-434 e428.

Zurborg S, Piszczek A, Martinez C, Hublitz P, Al Banchaabouchi M, Moreira P, Perlas E & Heppenstall PA. (2011). Generation and characterization of an Advillin-Cre driver mouse line. *Mol Pain* **7,** 66.

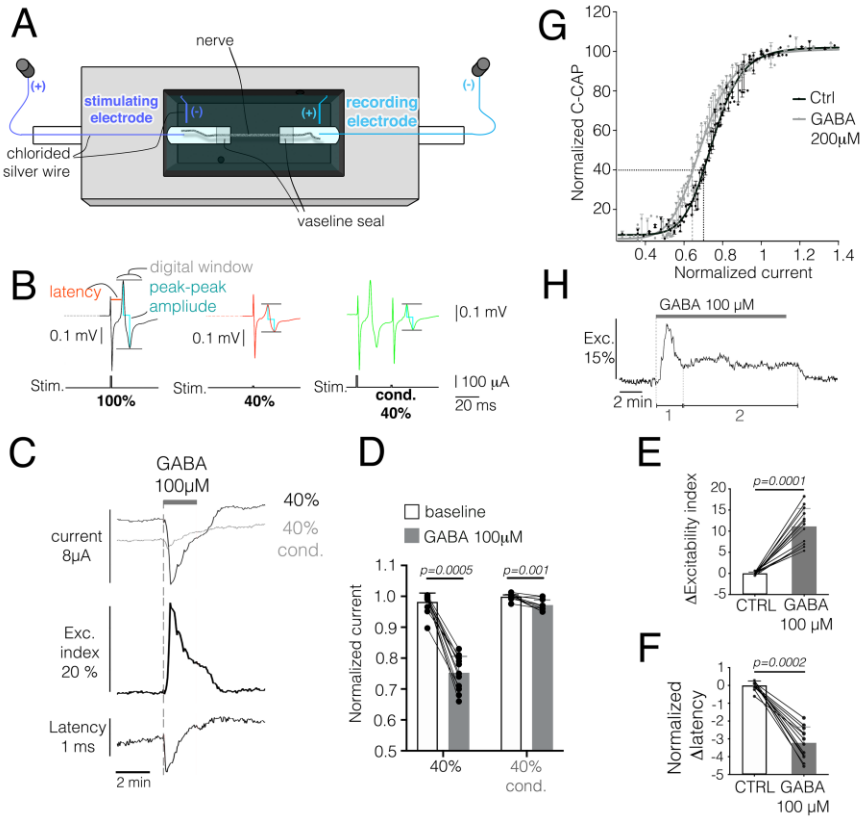

Figure 1

Figure 1. GABA increase electrical excitability of sural nerve C-fibres

A, Experimental configuration for electrical threshold tracking of C-fibre compound action potentials (C-CAP). Action potentials generated at the cathode (+) in response to constant current stimulation traverse the bath and are recorded extracellularly across a Vaseline sealing resistance. B, a rolling sequence of three stimulus conditions (1,2,3,1,2,3…) were used to track electrical threshold and thus excitability. Stimulus 1 (B, left-most trace) was set at 100µA (i.e. supra-maximal) to excite all axons and evoke a maximal (100%) C-CAP. The current strength for stimulus 2 was adjusted continuously by the QTRAC software aiming to maintain a C-CAP of 40% amplitude (B, 40% centre trace), i.e. an amplitude equal to 40% of the C-CAP response evoked by the preceding stimulus 1. Stimulus 3 was also adjusted by QTRAC to evoke a 40% C-CAP 30 ms after a preceding supra-maximal conditioning stimulus (B, 40% cond. right-most trace). C, the 1,2,3,1… sequence was repeated continuously. The stimulus current for the 40% and 40% conditioned stimuli (C, upper traces), the excitability index (C, centre trace and Eg.1) and the latency of 100% C-CAP (C, lower trace) were monitored over time. D,E,F, Application of GABA (100 µM, 2 min) reduced the current strength required to evoke the unconditioned 40% C-CAP and the conditioned 40% C-CAP (C, upper traces and D; n=12; 40% baseline vs. GABA Wilcoxon:

P=0.0005; 40% cond. Baseline vs. GABA Wilcoxon *P*=0.001) and thus increased the excitability index (C, centre trace and E; n=13; K-S D(ctrl)= 0.1084; D(GABA)= 0.1726; Wilcoxon: *P*=0.0001, n=13). F, GABA (100μM) also decreased C-CAP latency (n=12; D(ctrl)=0.1820; D(GABA)=0.1437; Wilcoxon : *P*=0.0002). *G*, Stimulus-response curve is shifted left-ward to lower current strengths by GABA (200 μM) resulting in a decrease in stimulus current required to evoke a C-CAP of any amplitude. The 40% C-CAP is indicated by the horizontal broken line (n=4; Sigmoid fit: df(ctrl)=143, df(GABA)=166; R^2 (ctrl)=0.9873, R^2 (GABA)=0.9836; EC_{50}(ctrl)=74.80±0.59, EC_{50}(GABA)=69.1±0.69). *H*, GABA (100 μM, 10 min) responses during sustained application were characterized by an initial transient phase 1 (of variable duration) and a subsequent sustained component that persisted during GABA application (phase 2).

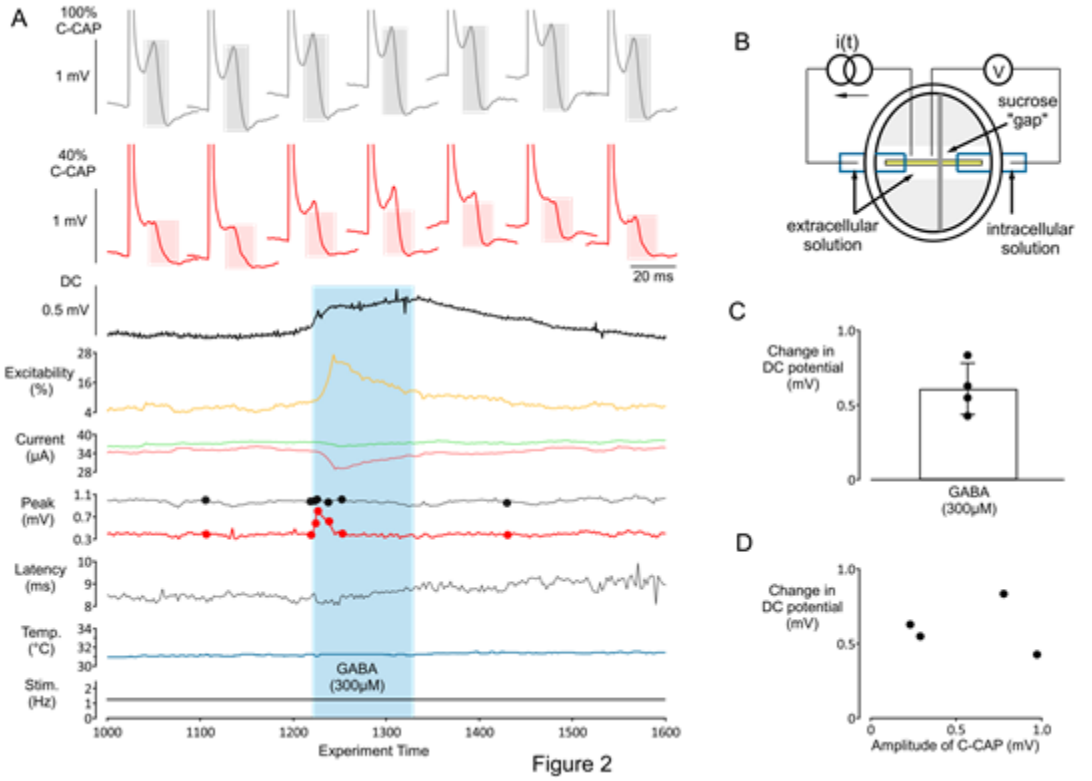

Figure 2. GABA depolarised axons in sural nerve

A, DC recording of electrical threshold tracking of C-fibre compound action potentials (C-CAP) during application of GABA (300 μM) using a sucrose gap configuration (B). At constant stimulus rate (A, lower trace) and constant temperature (A, second to lowest trace) GABA (A, shading) increases electrical excitability (A, excitability trace) owing to a reduction in the current required to maintain a 40% C-CAP (A, Current). During GABA application, the amplitude of the C-CAP (A, insets 40% C-CAP) to the prevailing stimulus strength aimed to generate a 40% C-CAP (A, Peak) increased. The increase in 40% C-CAP coincides with axonal depolarisation (A, upper trace). The current required to evoke a conditioned 40% C-CAP is not altered (A, Current). The C-CAP amplitude to supra-maximal stimulation remains unaltered throughout (A, upper insets 100% C-CAP and Peak trace). B, recording configuration to measure DC potential. The nerve (B, shaded horizontal bar) is secured at each end inside glass electrodes, one to stimulate at constant current (B, i(t) left) and the other to record (B, V right). DC recordings are made between the segment of nerve bathed in intracellular solution (B, right) and the centre compartment of the bath containing extracellular solution over a high resistance gap generated by extracellular sucrose (B, sucrose gap). C, pooled data for DC voltage change during GABA (n=4, mean=0.609 mV, sdev=0.171 mV). D, the magnitude of the voltage change during GABA is not dependent upon the amplitude of the electrically-evoked 100% C-CAP.

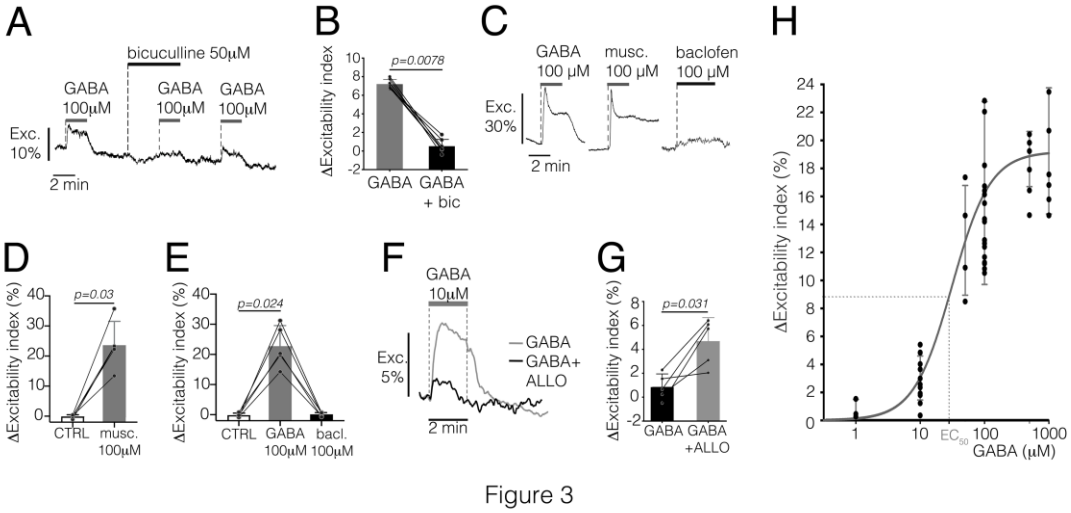

Figure 3

Figure 3. C-fibre excitability response to GABA are mediated by $GABA_AR$

A, axonal excitability responses to GABA (100 μM, 2 min) were blocked reversibly by the competitive $GABA_AR$ antagonist bicuculline (50 μM). B, pooled data for bicuculline blockade of GABA responses (n=7; D(GABA)= 0.22, D(GABA+bic)=0.24; Wilcoxon: p=0.0078, n=7). C, an increase in electrical excitability was observed in response to GABA (100 μM, 2 min, left) and the $GABA_AR$ agonist muscimol (100 μM; 2 min, centre) but not the $GABA_B$ agonist baclofen (100 μM; 4 min, right). D, pooled data for muscimol (n=5, D(ctrl)=0.34, D(mus)=0.32; Wilcoxon: p=0.03; n=5). E, pooled data for baclofen (n=4, W(ctrl)= 0.86, W(GABA)= 0.94, W(bacl)= 0.94; Friedman: df=(2,4), p=0.023; χ^2=5.99; post-hoc Dunnett: ctrl vs GABA p=0.024, ctrl vs baclofen p=0.99). F, axonal excitability responses to low concentrations of GABA (10 μM, 2 min) were enhanced by co-application of the neuroactive steroid ALLO (ALLO, 1 μM; 10 min pre-treatment). G, pooled data for co-application of GABA and ALLO (n=5; D(GABA)=0.17, D(GABA+ALLO)= 0.30; Wilcoxon, p=0.0312, n=5). H, GABA increased axonal excitability in a concentration-dependent manner with an EC_{50} of 31.28±18.88 μM (n=61; Sigmoid fit; df=58; R^2 0.7119).

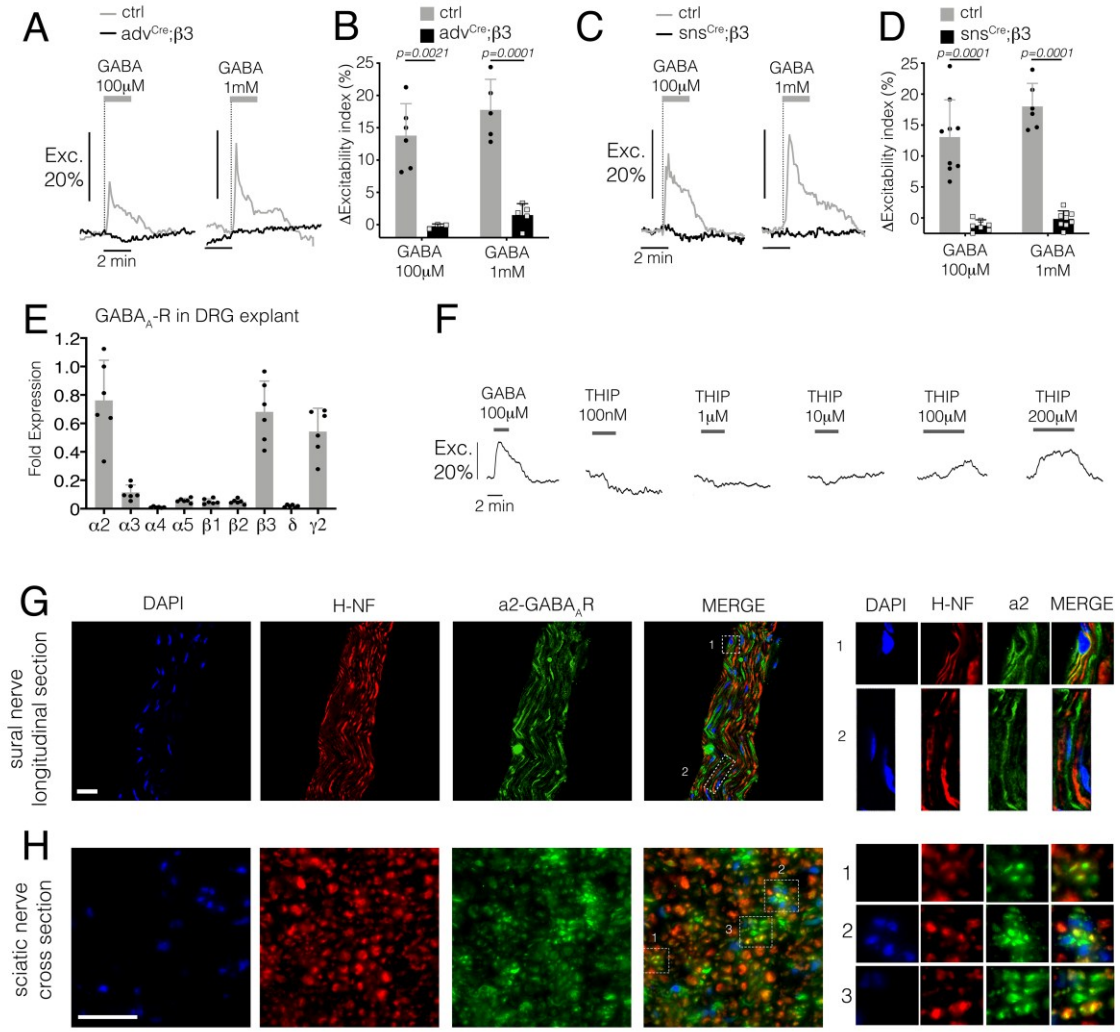

Figure 4

Figure 4. GABA$_A$R subunit characterization in DRG and peripheral axons

Axonal excitability responses to GABA at 100 μM (A-D, left) and 1 mM (A-D, right) were absent in *Adv^{Cre};β3^{flfl}* (A&B) and *sns^{Cre};β3^{flfl}* (C&D) null mice. B, pooled GABA response amplitude for *Adv^{Cre};β3^{flfl}* (panel B, n(ctrl$_{100\mu M}$)=6, n(Adv;β3$_{100\mu M}$)=3, W(ctrl$_{100\mu M}$)=0.95, W(Adv;β3$_{100\mu M}$)=0.80; unpaired t-test: p=0.002, df=7; n(ctrl$_{1mM}$)=5, n(Adv;β3$_{1mM}$)=5, D(ctrl$_{1mM}$)= 0.19, D(Adv;β3$_{1mM}$)= 0.2594; unpaired t-test: p=0.0001, df=8) and *sns^{Cre};β3^{flfl}* mice (panel D, n(ctrl$_{100\mu M}$)=9, n(sns;β3$_{100\mu M}$)=7, D(ctrl$_{100\mu M}$)= 0.20, D(Adv;β3$_{100\mu M}$)=0.18, unpaired t-test: p=0.0001, df=14; n(ctrl$_{1mM}$)=6, n(Adv;β3$_{1mM}$)=9, D(ctrl$_{1mM}$)=0.20, D(Adv;β3$_{1mM}$)=0.13, unpaired t-test: p=0.0001, df=13. E, mRNA transcript levels for GABA$_A$R subunits α2, α3, α4, β1, β2, β3, δ and γ2 shown relative to the housekeeping genes α-tubulin and 18s. F, axonal C-fibre excitability responses to THIP/gaboxadol at

concentrations from 100 nM to 200 μM following an initial GABA (100 μM; 2 min) application. THIP increased excitability at concentrations above 100 μM suggesting a lack of δ subunit containing $GABA_AR$. G&H, immunolabelled mouse sural nerve in longitudinal section (G) and sciatic nerve in cross-section (H). Preparations were co-stained for DAPI (blue, left), heavy neurofilament (H-NF, red, second from left), $GABA_AR$ α2 (green, third from left) and merged images (right) indicate α2 in both unmyelinated (green signal) and myelinated axons (yellow signal, co-localization with H-NF). Scale bars 20 μm G&H right, insets 1, 2 and 3 indicate expanded ROIs (white broken line rectangles) from merge.

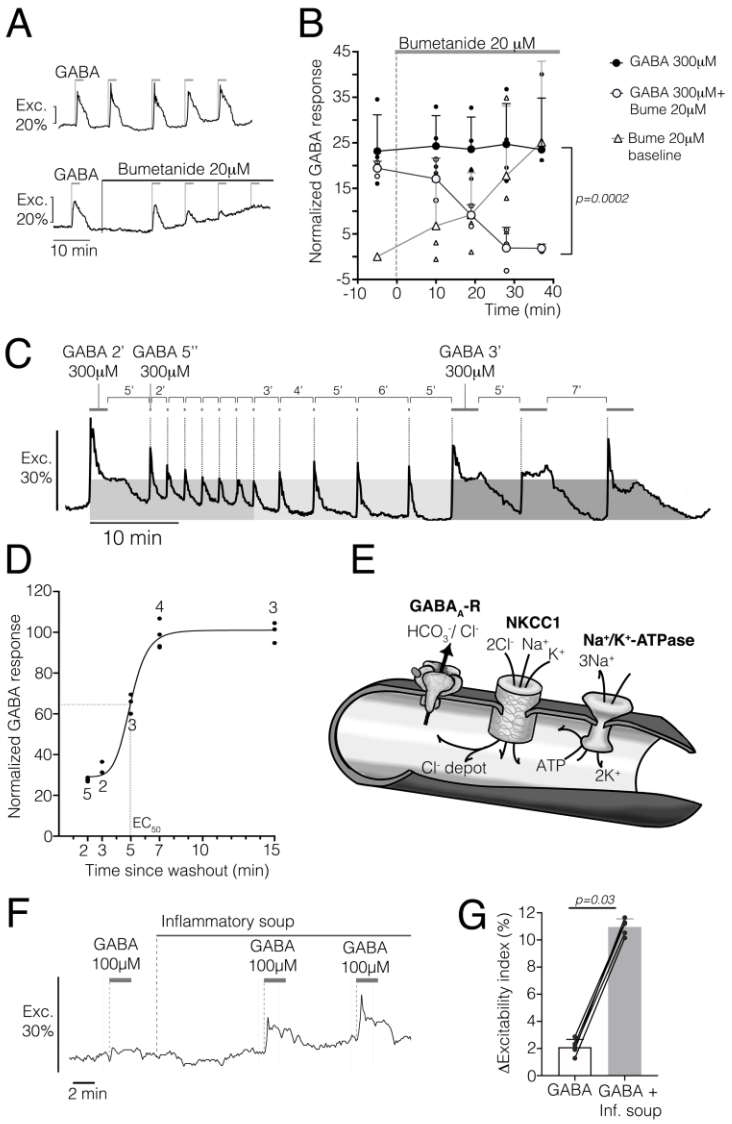

Figure 5

Figure 5. NKCC1 determined the amplitude of GABA-evoked excitability increase

A, repeat application of GABA (300 μM; 2 min) evoked reproducible increases in C-fibre excitability (A, upper trace). NKCC1 blockade with bumetanide (20 μM) increased excitability and resulted in a progressive reduction in GABA response amplitude (A, lower trace). B pooled data for repeat GABA (filled circles; n=6, D(GABA)=0.22, RM-ANOVA F(4,20)=1.16, p=0.358), the reduction of GABA response during bumetanide (open circles, n=3, D(GABA+bume)=0.23, RM-ANOVA, F(2,8)= 21.76, p=0.0002) and bumetanide's effect on excitability (open triangles, n=3, D(baseline)=0.21; RM-ANOVA F(2,8)=2.11, p=0.172). C, excitability responses to repeat GABA application. Following an initial GABA (300 μM, 2min), repeat 5sec GABA applications at 2 min intervals show a progressive decline in amplitude (C, grey shading, left). GABA response size recovers upon increasing

the interval between successive GABA (300 μM, 5 sec) applications from 2 min to 6 min (C, light grey shading, centre). Subsequent GABA (300 μM, 3 min) applications produce response comparable with the initial GABA response (dark grey shading, right). D, recovery of GABA response over time after preceding GABA application (n(2,3,5,7,15 min)=5,2,3,4,3; Sigmoid fit: xhalf=4.88±0.42, df=13). E, schematic indicating proposed coupling of Na^+/K^+-ATPase, NKCC1 and $GABA_AR$. F, axonal excitability responses to GABA (100 μM; 2 min) before and during inflammatory soup (histamine 1 μM, bradykinin 2 μM, PGE2 1 μM and serotonin 1 μM). G, Pooled data for GABA response before and during inflammatory soup (n=5, D(GABA)=0.18, D(GABA+IS)=0.26; Wilcoxon: p=0.03).

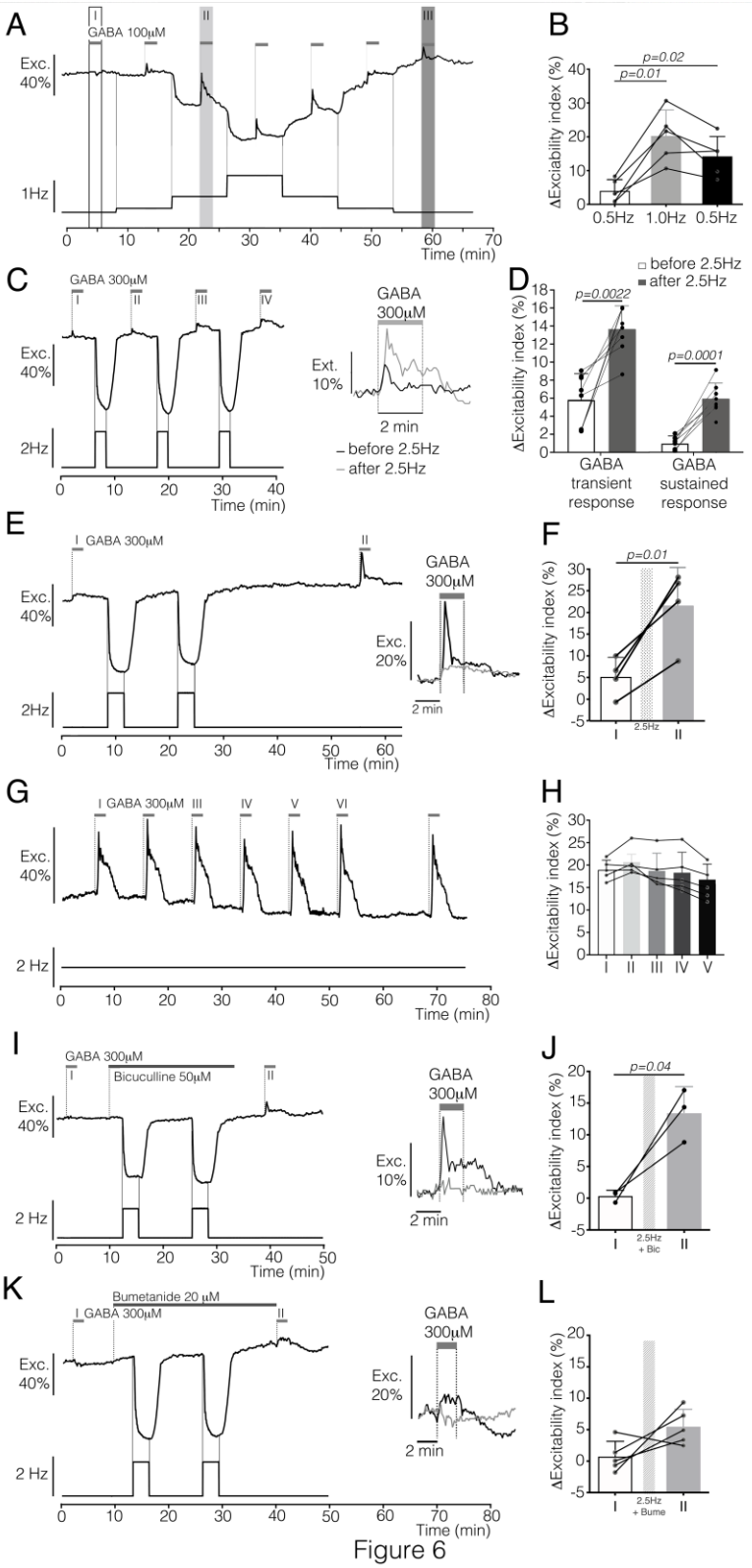

Figure 6

Figure 6. NKCC1 required for action potential dependent increase in GABA excitability response

A**,** axonal response to GABA (100 μM; 2 min, upper trace) increased as electrical stimulus rate increased step-wise from 0.5 to 1.7 Hz (lower trace). B, pooled data indicates elevated

GABA response persisted upon returning to the initial stimulus rate of 0.5Hz (n=5; $D(0.5Hz_{before})$=0.21, D(1Hz)=0.17, $D(0.5Hz_{after})$=0.20; RM-ANOVA, F(1.74,6.96)=23.57, p=0.0009 post-hoc Bonferroni: $0.5Hz_{before}$ vs. 1Hz p=0.013, $0.5Hz_{before}$ vs. $0.5Hz_{after}$ p=0.02). C, axonal response to GABA (300μM, 2 min, upper trace) increased following repeat bouts of electrical stimulation (2.5Hz, 3min, lower trace). C, inset shows overlay of first (I) and last (IV) response to GABA (300μM, 2min) D, pooled data for change in transient (n=8, D(before)=0.24, D(after)=0.19; paired t-test: p=0.002) and sustained component of GABA response following 2 or more bouts of electrical stimulation (2.5Hz, 3min; n=8, D(before 2.5Hz)=0.16, D(after 2.5Hz)=0.16; paired t-test: p=0.0001). E, elevated response to GABA (300 μM, 2 min, upper trace) persisted for over 30 minutes following 2 bouts of electrical stimulation (2.5 Hz, 3min, lower trace). E, inset shows overlay of GABA responses (I and II) and F shows pooled data (n=4, W(I)=0.98, W(II)=0.84; paired t-test: p=0.015). G, GABA response (300 μM; 2 min, upper trace) not changed by repeat application at 7 min intervals (GABA I-VI) . H, pooled data for repeat GABA (300μM, 2min; n=5; D(I)= 0.12, D(II)=0.31, D(III)=0.27, D(IV)=0.24; RM-ANOVA, F(1.8,7.2)=3.08, p=0.11). I, enhancement of response to GABA (300 μM; 2 min, upper trace) following bouts of electrical stimulation (2.5Hz, 3min, lower trace) not affected by $GABA_AR$ blockade with bicuculline (50 μM). J, pooled data for effect of bicuculline (n=3; W(I)= 0.82, W(II)=0.96; paired t-test: p=0.04). K, NKCC1 blockade with bumetanide (20 μM) reduces enhancement of response to GABA (300 μM, 2 min, upper trace) following bouts of electrical stimulation (2.5Hz, 3min, lower trace). L, pooled data for bumetanide (20μM; n=5; D(I)=0.21, D(II)=0.18; paired t-test: p=0.10).

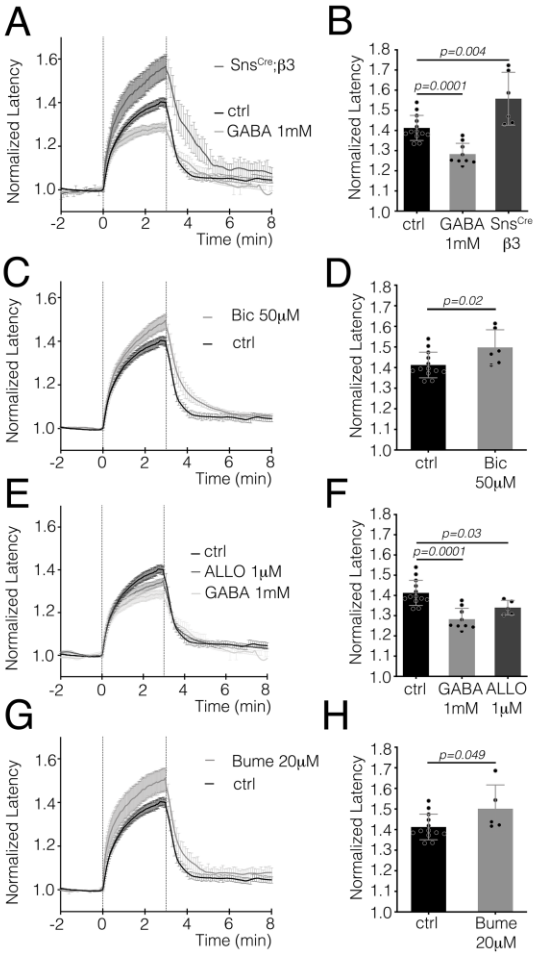

Figure 7

Figure 7. $GABA_AR$ modulation of activity-dependent slowing in C-fibres

Electrical stimulation at 2.5 Hz for 3 min produced activity-dependent slowing (ADS) of axonal conduction velocity that was measured as an increase in C-CAP latency (A, ctrl). A, ADS was enhanced in $sns^{Cre};\beta3^{-/-}$ mice (A, dark grey trace) and reduced by the application of GABA (1 mM, light grey trace). B, pooled data for ADS over the last 30 sec of 2.5 Hz stimulation (n(ctrl)=13, n(GABA)=9; D(ctrl)=0.2245, D(GABA)=0.2689; ctrl vs GABA, unpaired t-test, p=0.001 ; n($sns^{Cre};\beta3$)=6, D($sns^{Cre};\beta3$)=0.2497, ctrl vs $sns^{Cre};\beta3$, unpaired t-test: p=0.004). C, ADS was increased in the presence of the $GABA_AR$ antagonist bicuculline (50 μM, grey trace); D, pooled data for bicuculline (50μM; n(ctrl)=13, n(bic)=6; D(ctrl)=0.22, D(bic)=0,25; unpaired t-test, p=0.024). E, ADS was reduced by co-application of GABA and the positive allosteric modulator ALLO (grey trace). F pooled data for co-application of GABA (1mM) and ALLO (1μM; n(ctrl)= 13, n(GABA+ALLO)=5; D(ctrl)=0.22, D(GABA+ALLO)=0.21; ctrl vs. GABA+ALLO unpaired t-test, p=0.027). G, NKCC1 blockade by bumetanide (20 μM, grey trace) increased ADS. H, pooled data (n(ctrl)=13, n(bume)=5; D(ctrl)=0.22, D(bume)=0.31; unpaired t-test, p=0.049).

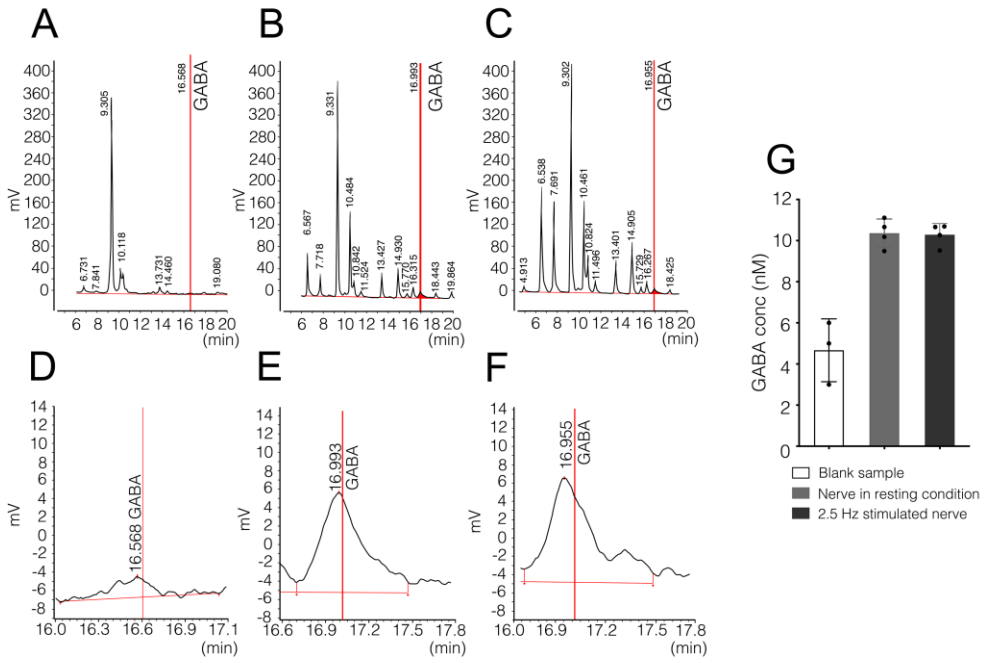

Figure 8

Figure 8. HPLC determination of GABA in solution bathing sural nerve

HPLC chromatograms indicating GABA (vertical red line) in a blank sample of extracellular HEPES buffered physiological solution (A), extracellular HEPES buffered solution in which a segment of sural nerve was bathed for 15 min (B) and HEPES buffered solution in which a segment of sural nerve was bathed and stimulated electrically at 0.5Hz with two bouts at 2.5 Hz each for 3 minutes (C). D-F, expanded region of chromatograms A-C over the GABA elution time zone. G, GABA concentration in HEPES solution alone (open bar, n=3; 4,67±1,53 nM), with a sural nerve but without electrical stimulation (grey, n=4; 10.36±0.69 nM) and during electrical stimulation (black, n=4; 10.28±0.54 nM). There was no difference in GABA concentration for the bathing solution with and without electrical stimulation (unpaired t-test, p=0.56)

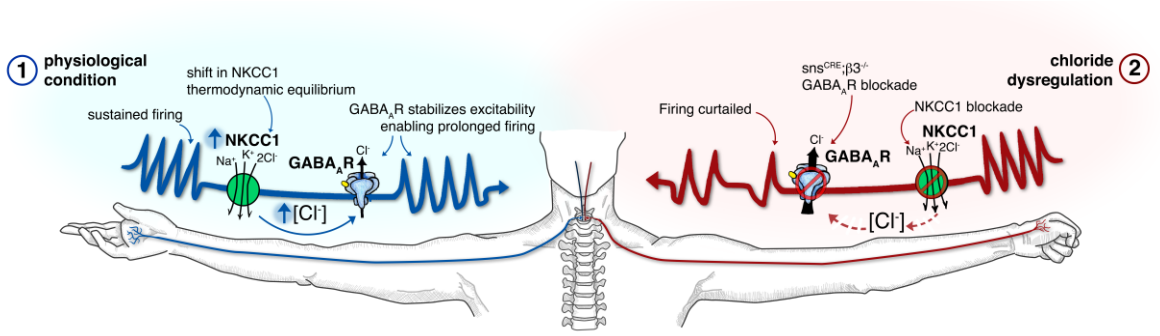

Figure 9

Figure 9. Schematic summary of possible role of $GABA_AR$ in unmyelinated axons

1, Under physiological conditions sustained firing results in a feed-forward loading of intra-axonal chloride via NKCC1 . The chloride gradient allows a chloride conductance, eg. $GABA_AR$, to stabilise axonal excitability and enable prolonged firing. 2, chloride dysregulation resulting from either NKCC1 blockade, $GABA_AR$ inhibition or deletion ($sns^{Cre};\beta3^{-/-}$) exacerbates activity-dependent slowing and the ability to sustain firing is curtailed.

Table 1. Primers sequences

Primer Name	Forward primer 5'-3'	Reverse primer 3'-5'
RAα2	GTATTACTGAAGTCTTCACTAACATT	CGAAAGAAAACATCTATTGTATACTCCATATC
RAα3	GCCCACTGAAGTTTGGAAGCTATG	ACTGATTCAGGCGTGAGCCATC
RAα4	TCCTGGATTTGGGGGTCCTGTTA	TCAACATCAGAAACGGGCCCA
RAα5	TCCCAGGTGTCCTTTTGGCT	GCACTGTGGTCACTCCAAAAACTG
RAβ1	CTGCATCCGATGGAACTGTTC	CTCATCCAGAGGGTATCTTCGAA
RAβ2	TGCGCCTGGATGTCAACAAGATG	TGCTGGAGGCATCATAGGCAAG
RAβ3	AATCCTCTCGTGGGTGTCCTTC	TGAGCACGGTGGTAATCCCAAG
RAγ2	ACTTCGACCTGACATCGGAGTG	TCACTGGACCAATGCTGTTCAC
α-tubulin	TCGCGCTGTAAGAAGCAACACC	ATGGAGATGCACTCACGATGGT
18s	CTGCCCTATCAACTTTCGATGGTAG	CCGTTTCTCAGGCTCCCTCTC

Veronica Bonalume obtained her PhD in “Integrated Biomedical Research” at the University of Milan, Dept. of Pharmacological and Biomolecular Sciences, focusing on the study of the molecular pathways involved in peripheral neuron-glia interaction. During her PhD she worked in the laboratory of Dr. Richard Carr in the Experimental Pain Research Department at Heidelberg University, Germany. Currently, Veronica is Post-Doc researcher in the Dept. of Pharmacological and Biomolecular Sciences, University of Milan, within the group of Prof. Valerio Magnaghi.